Epigenetic Regulation of Lipid Metabolism in Neural Stem Cell Fate Decision

Charvi Syal

This thesis is submitted as a partial fulfillment of the M.Sc. program in Cellular and Molecular Medicine

Department of Cellular and Molecular Medicine

Faculty of Medicine

University of Ottawa

Ottawa, Canada

Abstract

Bioactive lipids have emerged as prominent regulators of neural stem and progenitor cell (NPC) function under both physiological and pathological conditions. However, how lipid metabolism is regulated, and its role in modulation of NPC function remains unknown. In this regard, my study defines a novel epigenetic pathway that regulates lipid metabolism to determine NPC proliferation versus differentiation. Specifically, I show that activation of an atypical protein kinase C (aPKC)-mediated Ser436 phosphorylation of CREB binding protein (CBP) by aging, metformin stimulation and continued passaging *in vitro*, represses expression of monoacylglycerol lipase (Mgll) to promote neuronal differentiation of adult NPCs. Mgll, a lipase that hydrolyzes the endocannabinoid 2-arachidonoyl glycerol (2-AG) to produce arachidonic acid (ARA), is thus a key regulator of two critical bioactive lipid signaling pathways in the brain and a potential modulator of NPC function. I observed elevated Mgll levels, concomitant with neuronal differentiation deficits in both the lateral ventricle sub-ventricular zone (SVZ) and the hippocampal subgranular zone (SGZ) NPCs of phospho-null CBPS436A mice, that lack a functional aPKC-CBP pathway. Genetic knockdown of Mgll or inhibition of Mgll activity rescued these neuronal differentiation deficits. In addition, I found that CBPS436A SVZ NPCs exhibit enhanced proliferation at the expense of differentiation as an outcome of increased Mgll levels in culture. Interestingly, I also observed that SVZ NPCs from an Alzheimer's disease (AD) model, the 3xTg mice, closely resemble CBPS436A NPC behaviour in culture. 3xTg NPCs exhibit attenuation of the aPKC-CBP pathway, which is associated with elevated Mgll expression and increased NPC

proliferation at the expense of neuronal differentiation. Reactivation of the aPKC-CBP mediated-Mgll repression in 3xTg AD NPCs mitigates their differentiation deficits.

These findings implicate Mgll as a critical switch that regulates NPC function by altering bioactive lipid signaling (2-AG versus ARA). They demonstrate that the aPKC-CBP mediated Mgll repression is essential for normal NPC function, and that when perturbed in AD, it causes impaired NPC function to generate fewer neurons, contributing to AD predisposition.

Table of Contents

Abstract ..... ***ii***

Table of Contents ..... ***iv***

List of Tables and Diagrams ..... ***vii***

List of Figures ..... ***viii***

List of Abbreviations ..... ***ix***

Acknowledgements ..... ***xii***

1. Introduction **1**

1.1. Adult Neurogenesis 1

1.2. Adult Neurogenesis and Lipid Metabolism 3

1.2.1. Bioactive Lipid Signaling in Adult Neurogenesis 5

A. Polyunsaturated Fatty Acid Signaling 5

B. Endocannabinoid Signaling 6

1.3. Alzheimer's Disease 9

1.3.1. Clinical Outcomes 10

1.3.2. Genetics and Risk Factors 10

1.3.3. Hallmarks and Pathology 11

1.3.4. Mouse Models of AD 12

1.4. Neurogenesis and Alzheimer's Disease 14

1.5. Lipid Metabolism and Alzheimer's Disease 16

1.6. Epigenetic Regulation of Neurogenesis and Alzheimer's Disease: Role of the aPKC-CBP Pathway 18

2. Hypothesis and Objectives **22**

2.1. Hypothesis 22

2.2. Objectives 22

3. Materials and Methods.....23

3.1. Animals.....23

3.2. NIH3T3 Cell Culture.....23

3.3. Adult Neurosphere Culture.....24

3.4. NPC Differentiation.....25

3.5. NPC Transfection and Conditioned Medium Treatment.....26

3.6. Neurosphere Size Assessment and GPR40 Antagonist Treatment.....27

3.7. Drug Treatment in Cultured NPCs.....27

3.8. Immunocytochemistry.....28

3.9. JZL-184 and 5-Bromo-2'-deoxyuridine (BrdU) Injections.....29

3.10. Tissue Preparation.....29

3.11. Immunohistochemistry.....30

3.12. Imaging and Quantification.....30

3.13. Western Blot.....31

3.14. Statistical Analysis.....33

4. Results.....34

4.1. Mgll expression is elevated in differentiating CBPS436A NPCs.....34

4.2. Genetic knockdown of Mgll rescues NPC differentiation deficits in CBPS436A NPCs *in vitro*.....37

4.3. Mgll inhibition rescues hippocampal neurogenesis deficits in CBPS436A mice *in vivo*.42

4.4. Late passage NPCs display intrinsic activation of the aPKC-CBP pathway.....45

4.5. 3xTg NPCs exhibit an impaired aPKC-CBP mediated Mgll repression.....48

4.6. The attenuation of aPKC-CBP mediated Mgll repression leads to increased NPC proliferation at the expense of their neuronal differentiation.....50

4.7. Mgll knockdown rescues neuronal differentiation deficits in late passage CBPS436A NPCs.....56

4.8. Reactivation of the aPKC-CBP mediated Mgll repression rescues differentiation deficits in 3xTg NPCs……58

5. Discussion……63

5.1. The aPKC-CBP pathway directly regulates Mgll expression……63

5.2. Mgll acts in cell intrinsic and cell extrinsic manners……64

5.3. Continued passaging of NPCs is a novel alternate model to study the aPKC-CBP-Mgll pathway ……65

5.4. Mgll promotes NPC proliferation at the expense of neuronal differentiation……67

5.5. The aPKC-CBP-Mgll pathway is impaired in 3xTg NPCs……68

6. Conclusion……70

7. References……71

Appendix……85

List of Tables and Diagrams

Diagram 1. Schematic overview of the study……..21

Diagram 2. Schematic summary of thesis……..70

Table 1. shRNA Sequences ……..85

Table 2. Medium and Reagents……..85

Table 3. List of Solutions……..86

List of Figures

Figure 1. Mgll is aberrantly upregulated in CBPS436A mice……20

Figure 2: CBPS436A NPCs exhibit elevated Mgll expression……35

Figure 3: CBPS436A NPCs exhibit elevated acetyl-H2B levels……36

Figure 4: Efficiency of shRNA-mediated Mgll knockdown……39

Figure 5: Mgll knockdown rescues neuronal differentiation deficits in CBPS436A NPCs in cell intrinsic and cell extrinsic manners……40

Figure 6: Inhibition of Mgll activity with JZL-184 rescues hippocampal neurogenesis deficits in CBPS436A mice……..43

Figure 7: Late passage CBPS436A NPCs display intrinsic activation of aPKC-CBP pathway……46

Figure 8: 3xTg NPCs display reduced aPKC levels and elevated Mgll levels……..49

Figure 9: Late passage CBPS436A P5 NPCs exhibit enhanced proliferation, concurrently with reduced differentiation ……52

Figure 10: Early passage 3xTg P2 NPCs exhibit enhanced proliferation, concurrently with reduced differentiation ……54

Figure 11: Mgll knockdown rescues neuronal differentiation deficits in late passage CBPS436A P5 NPCs……57

Figure 12: Reactivation of aPKC-CBP mediated Mgll repression rescues neuronal differentiation defects in 3xTg NPCs……60

Figure 13: The endocannabinoid pathway mediates neuronal differentiation in 3xTg NPCs……62

List of Abbreviations

2-AG	2-Arachidonoylglycerol
3xTg	Triple transgenic model of AD
Aβ	Amyloid beta
AD	Alzheimer's disease
AEA	N-arachidonoylethanolamine or anandamide
AMPK	(Adenosine monophosphate)-activated protein kinase
ANOVA	Analysis of variance
aPKC	Atypical protein kinase C
ApoE	Apolipoprotein E
ApoE4	Apolipoprotein E, allele ε4
ARA	Arachidonic acid
bFGF	Basic fibroblast growth factor
BrdU	5-Bromo-2'-deoxyuridine
BSA	Bovine serum albumin
CBP	CREB binding protein
CM	Conditioned medium
COX-2	Cyclooxygenase-2
CREB	cAMP response element binding protein
DCX	Doublecortin
DHA	Docosahexaenoic acid
DIV	Days *in vitro*
DMEM	Dulbecco's modified Eagle's medium
DMSO	Dimethyl sulfoxide
eCB	Endocannabinoid
eCBR	Endocannabinoid receptor
eCBR1	Endocannabinoid receptor 1
eCBR2	Endocannabinoid receptor 2
EGF	Epidermal growth factor
eGFP	Enhanced green fluorescent protein

F12	Ham’s F12 medium
FAAH	Fatty acid amide hydrolase
FAD	Familial Alzheimer’s disease
FASN	Fatty acid synthase
FBS	Fetal bovine serum
GAPDH	Glyceraldehyde 3-phosphate dehydrogenase
GFAP	Glial fibrillary acidic protein
GPCR	G-protein coupled receptor
GPR40	G-protein coupled receptor 40
H2B	Histone H2b
hAPP	Human amyloid precursor protein
HAT	Histone acetyltransferase
HBSS	Hank’s balanced salt solution
HRP	Horseradish peroxidase
hTau	Human tau
i.p.	Intraperitoneal
KI	Knock-in
LTP	Long term potentiation
Mgll	Monoacylglycerol lipase
MUFA	Monounsaturated fatty acid
NeuN	Neuronal nuclei
NFTs	Neurofibrillary tangles
NGS	Normal goat serum
NHS	Normal horse serum
Non-Tg	Non-transgenic mice
NPC	Neural precursor cell
NS	Neurosphere
NSC	Neural stem cell
OB	Olfactory bulb
P2	Passage 2
P5	Passage 5

PBS	Phosphate buffered saline
p-aPKC	Phosphorylated atypical protein kinase C
p-CREB	Phosphorylated cAMP response element binding protein
PFA	Paraformaldehyde
PLO	Poly-L-ornithine
PMD	Post-mortem delay
PMSF	Phenylmethylsulfonyl fluoride
PSA-NCAM	Polysialylated neural cell adhesion molecule
PS1	Presenilin-1
PS2	Presenilin-2
PUFA	Polyunsaturated fatty acid
SAD	Sporadic Alzheimer's disease
Scr	Scrambled
SDS	Sodium dodecyl sulfate
SFA	Saturate fatty acid
SFM	Serum-free medium
SFM+EFHB	SFM containing EGF, FGF, heparin and B27
SEM	Standard error of the mean
SGZ	Subgranular zone
shRNA	Short hairpin RNA
Sox2	(Sex determining region Y)-box 2
SVZ	Subventricular zone
TAp73	Transcriptionally active protein 73
TBS-T	Tris buffered saline, tween-20
T-aPKC	Total atypical protein kinase C
TF	Transcription factor
WT	Wildtype

Acknowledgements

I would like to first and foremost thank my supervisor, Dr. Jing Wang for providing me the opportunity to work on this exciting project. Dr. Wang, I am sincerely grateful to you for your consistent guidance and excellent mentorship. I consider myself fortunate to have had a supervisor who is so approachable and willing to answer any and all questions. I am especially thankful to you for your endless patience and unyielding support during my initial few months in Canada and during a particularly challenging time last summer. This M.Sc. would not have been possible without you.

I also want to extend my thanks to all the current and past members of the Wang Lab especially: Jacob Thomas, Matthew Seegobin, Sailendra Nath Sarma, Jayasankar Kosaraju, Ayden Gouveia and Fares Ould-Brahim, for all their help. Jacob and Matthew, I sincerely appreciate your thorough work and continuous support when I needed it the most.

I would also like to thank my thesis advisory committee members, Dr. David Picketts and Dr. Steffany Bennett, for their critical insight during our meetings and for their valuable input that has helped shape my thesis.

Lastly, I would like to thank my parents, who despite being more than 10,000 kilometers away were my biggest support throughout. Mom and Dad, this thesis would not have been possible without your constant encouragement and unfailing confidence in me.

1. Introduction

1.1. Adult Neurogenesis

The adult mammalian brain was once considered a static, post-mitotic organ that lacked the ability of regeneration. However, the pioneering study by Altman and Das in the 1960s challenged this view, when they successfully demonstrated the generation of new neurons in the adult rat hippocampus using ^{3}H-thymidine incorporation (Altman and Das, 1965). Since this initial discovery, multiple studies have provided compelling evidence in support of sustained production of new neurons in the brain throughout adulthood, termed adult neurogenesis (Lois and Alvarez-Buylla, 1993; Kempermann *et al.*, 1997).

Adult neurogenesis arises from adult neural stem cells (NSCs) that reside primarily in two neurogenic niches, the subventricular zone (SVZ) of the lateral ventricles and the sub-granular zone (SGZ) of hippocampal dentate gyrus (DG) (Imayoshi *et al.*, 2008; Zhao *et al.*, 2008; Kuhn *et al.*, 2016). Increasing evidence suggests that neurogenesis also occurs in other brain regions, such as the striatum, neocortex, and hypothalamus. However, these findings remain controversial and require further investigation (Rakic, 2002; Pierce *et al.*, 2010; Ernst *et al.*, 2014). NSCs are Sox2 and glial fibrillary acidic protein (GFAP) expressing cells that possess the ability to self-renew and to differentiate into all three neural lineages: neurons, astrocytes and oligodendrocytes. These NSCs give rise to neural progenitor cells, also called transient amplifying cells. Both NSCs and neural progenitors express the intermediate filament protein, nestin, and are collectively termed as neural precursor cells (NPCs). Adult NPCs in both the SVZ and SGZ predominantly differentiate into neuroblasts that express doublecortin (DCX) and polysialylated

neural cell adhesion molecule (PSA-NCAM). These neuroblasts migrate and form neuronal nuclei (NeuN) expressing mature neurons in the olfactory bulb and granular cell layer of hippocampus, respectively (Zhao *et al.*, 2008). Both SVZ and SGZ neurogenesis support distinct physiological functions in the adult brain. On the one hand, SGZ-derived neuroblasts form excitatory granule neurons that incorporate into the existing DG circuitry, receive inputs from the entorhinal cortex while projecting axons to the CA3 region of the hippocampus (Zhao *et al.*, 2008), and thus participate in hippocampal-associated learning and memory (Imayoshi *et al.*, 2008; Zhao *et al.*, 2008). On the other hand, SVZ-derived neuroblasts, in the rodent brain, traverse the rostral migratory stream to form interneurons in the olfactory bulb (OB) and participate in OB sensory function (Imayoshi *et al.*, 2008).

In the late 1990's Eriksson et al. for the first time provided evidence in support of the birth of hippocampal neurons in humans (Eriksson *et al.*, 1998). This was further validated when Spalding et al. used ^{14}carbon birth-dating of neuronal DNA to provide a convincing evidence of adult neurogenesis in humans (Spalding *et al.*, 2013). However, two recent studies have now rekindled the debate regarding the existence of adult neurogenesis in humans by reporting opposing findings (Sorrells *et al.*, 2018; Boldrini *et al.*, 2018). While Sorrells et al. showed that hippocampal neurogenesis in humans drops sharply with age to nearly undetectable levels in adults, Boldrini et al. concluded that adult neurogenesis persists lifelong (Sorrells *et al.*, 2018; Boldrini *et al.*, 2018). Both studies performed histological analysis of early neuronal markers DCX and PSA-NCAM. However, while Sorrells et al. observed no expression of these neuronal markers in post-mortem adult brain tissues, Boldrini et al. reported an extensive expression of the same markers in their study. This disparity can be attributed to the different methodologies used by

the two groups, and importantly to the post-mortem delay (PMD) in tissue fixation. Previous studies have demonstrated the susceptibility of DCX to rapid degradation following death (Boekhoorn *et al*., 2006), which may explain the lack of DCX staining in the Sorrells et al. study, where PMD in sample fixation was quite long (up to 48 hours), while in the Boldrini et al. study PMD was relatively shorter (<26 hours). Furthermore, Sorrells et al. included some epilepsy tissues in their study, which are not ideal for neurogenesis assessments as previous work has demonstrated significant neurogenic impairments following epilepsy (Jessberger and Parent, 2015). In contrast, Boldrini et al. excluded subjects with any known history of neurological or psychiatric disorders.

Despite these recent controversial findings, there is a large body of evidence, accumulated over the years, arguing the existence of adult neurogenesis in both the rodent and human brain. More comprehensive analyses using advanced techniques such as a single cell transcriptomic approach and *in vivo* imaging will help to clarify the controversial view regarding adult neurogenesis; however, currently, there is no reason to doubt the existence of adult neurogenesis in humans (Kempermann *et al*., 2018).

1.2. Adult Neurogenesis and Lipid Metabolism

Adult neurogenesis is an intricate, multistep process that involves coordinated NPC proliferation, differentiation, migration, and incorporation of the newborn neurons into a functional neuronal circuitry. Each step of this complex process is tightly regulated by a variety

of intrinsic factors and extrinsic cues including signaling cascades, transcriptional factors, and epigenetic regulators (Bond *et al.*, 2015). Interestingly, increasing evidence now supports a role of lipid metabolism in regulating adult neurogenesis (Knobloch and Jessberger, 2017; Knobloch 2017).

Lipids are multifaceted molecules that make up more than half of the adult brain's dry weight. This diverse class of macromolecules, with an estimated 100,000 distinct types in humans, play many crucial roles in the adult brain (Shevchenko and Simons, 2010). Lipids form chief structural components of cell membranes and provide a rich source of energy. Most importantly, however, they participate in intracellular and extracellular signaling as bioactive lipids (Shevchenko and Simons, 2010; Hussain *et al.*, 2013). The central role of lipids in the regulation of adult neurogenesis was recently recognized when a landmark study demonstrated that fatty acid synthase (FASN)-dependent *de novo* lipogenesis was critical for adult NPC proliferation, and that inhibition of this process promoted NSC quiescence (Knobloch *et al.*, 2013). In agreement with this study, another research work showed that exercise-enhanced NPC proliferation and cognition was abolished upon inhibition of FASN (Chorna *et al.*, 2013). Furthermore, increasing studies have now reported that genes involved in lipid biogenesis and metabolism are richly expressed in NSCs, suggesting a critical role of lipids in regulating NSC function (Shin *et al.*, 2015; Codega *et al.*, 2014; Llorens-Bobadilla *et al.*, 2015; Hamilton and Fernandes, 2018).

In addition to these physiological roles of lipid metabolism in regulating NSC function, a recent study revealed that an abnormal build-up of lipids in the SVZ niche was associated with

Alzheimer's disease (AD) (Hamilton *et al.*, 2015). The authors showed that aberrant accumulation of lipid droplets in the ependymal cells, a key component of the SVZ niche, suppressed NPC proliferation in an AD mouse model (Hamilton *et al.*, 2015).

These findings thus indicate that lipid metabolism plays a critical role in regulating NPC function under both physiological and pathological conditions.

1.2.1 Bioactive Lipid Signaling in Adult Neurogenesis

Bioactive lipids, with distinct cell signaling roles, have recently emerged as important regulators of adult neurogenesis (Bieberich, 2012). A variety of bioactive lipids, by binding to their specific receptors, transduce critical signaling cascades which can modulate NPC function.

A. Polyunsaturated Fatty Acid Signaling

Polyunsaturated fatty acids (PUFAs) including omega-3 (docosahexaenoic acid; DHA) and omega-6 (arachidonic acid; ARA) fatty acids are well known for their beneficial effects in regulating NSC function both during development and adulthood (Beltz *et al.*, 2007; Sakayori *et al.*, 2011; Tokuda *et al.*, 2014). DHA, an important omega-3 fatty acid, has been shown to promote neurogenesis both *in vivo* and *in vitro*, as well as support memory formation (He *et al.*, 2009; Kawakita *et al.*, 2006). Further, dietary supplementation of DHA is known to improve synaptic plasticity and cognition (Wu *et al.*, 2008; He *et al.*, 2009). In addition, the omega-6 PUFA, ARA, has also been shown to promote NPC proliferation and drive neurogenesis (Maekawa *et al.*, 2009; Tokuda *et al.*, 2014). ARA is a major precursor for the generation of pro-inflammatory molecules such as prostaglandins, thromboxanes, and leukotrienes, collectively called eicosanoids (Khanapure *et al.*, 2007). The ARA-induced NSC proliferation is attributed partly to

the eicosanoid-activated signaling, and partly to direct ARA signaling through free fatty acid binding receptors, such as the GPR40 (also called free fatty acid receptor 1, FFA1) (Kang *et al.*, 2014; Boneva and Yamashima, 2012; Lichtenwalner and Parent, 2006; Yamashima, 2012; Bieberich, 2012). ARA-GPR40 signaling promotes both NPC proliferation and neurogenesis in the ischemic primate brain by activating cAMP response element binding protein (CREB) (Boneva and Yamashima, 2012). Since GPR40 is abundantly expressed in the primate brain, most of the initial GPR40 studies were restricted to primates (Boneva and Yamashima, 2012). However, a recent study demonstrated a significant expression of GPR40 in murine hippocampal neurons, thus suggesting that mice represent a suitable model for elucidating the role of GPR40 signaling in brain function (Zamarbide *et al.*, 2014).

B. Endocannabinoid Signaling

Another important class of bioactive lipids that modulate NSC function is the endocannabinoids (eCB). The endocannabinoid (eCB) system is involved in a range of physiological brain functions such as pain, emotion, memory and behavioural responses (Lu and Mackie, 2015). The eCB system comprises of endogenous ligands (eCBs), their binding receptors (eCBRs), and enzymes regulating eCB synthesis and breakdown.

Anandamide (AEA) and 2-arachidonoyl glycerol (2-AG) are the two best-characterized eCBs in the brain. The eCB lipids are produced in an activity-dependent manner from membrane phospholipids by enzymatic cleavage (Di Marzo *et al.*, 2015). The eCBs act as retrograde synaptic messengers that are released by post-synaptic neurons and bind to eCBRs localized on pre-synaptic neurons to stimulate neurotransmitter release. While 2-AG is a high efficacy agonist that

activates both eCBR1 and eCBR2, AEA behaves as a partial agonist with low efficacy at both the eCBRs (Di Marzo *et al.*, 2015; Lu and Mackie, 2015; Di Marzo and De Petrocellis, 2012).

The two eCBRs, eCBR1 and eCBR2, are G-protein coupled receptors (GPCRs) that transduce eCB signaling effects by inhibition of adenylyl cyclases and voltage-gated calcium channels and activation of MAP kinases and inwardly-rectifying potassium channels (Di Marzo *et al.*, 2015; Fonseca *et al.*, 2013). Of the two, eCBR1 is dominantly expressed in neurons in the brain cortex, hippocampus, basal ganglia and the cerebellum (Di Marzo *et al.*, 2015; Lu and Mackie, 2015), and mediates most of the physiological functions of the eCB system. In contrast, eCBR2 expression level is very low in the brain and is mainly restricted to astrocytes, microglia and vascular elements, implicating a role in inflammation (Di Marzo *et al.*, 2015; Kendall and Yudowski, 2017). However, under several neuropathological conditions, expression of eCBR2 is markedly increased and is also observed in neurons (Lu and Mackie, 2015). Given its involvement in neuroinflammatory processes, eCBR2 has recently emerged as a potential target against different neuropathological conditions, including AD (Cassano *et al.*, 2017; Aso and Ferrer, 2016; Bonnet and Marchalant, 2015).

The role of eCB signaling in regulating NPC function and neurogenesis has been widely studied. These studies have demonstrated a critical role of eCB signaling in regulating diverse NPC functions such as self-renewal and neuronal differentiation and maturation during both embryonic and post-natal stages (Maccarrone *et al.*, 2014; Galve-Roperh *et al.*, 2013). Signaling through both eCBR1 and eCBR2 has been extensively shown to promote NPC proliferation (Galve-Roperh *et al.*, 2013; Palazuelos *et al.*, 2006, 2012; Jin *et al.*, 2004b). Importantly, the role of eCBR1

and eCBR2 signaling in driving neuronal differentiation of NPCs has also been demonstrated (Jin *et al.*, 2004b; Díaz-Alonso *et al.*, 2012; Xapelli *et al.*, 2013; Compagnucci *et al.*, 2013; Bravo-Ferrer *et al.*, 2017). These effects are potentially mediated by 2-AG, since both genetic ablation and inhibition of diacylglycerol lipase α (DAGLα), the primary 2-AG producing enzyme, have been shown to result in significant deficits in both, SVZ and hippocampal neurogenesis (Gao *et al.*, 2010; Goncalves *et al.*, 2008).

The third important component of the eCB system is the enzymes that mediate eCB hydrolysis and synthesis. The eCB hydrolases, by breaking down eCBs, can effectively stop eCB signaling and are thus a critical regulator of eCB signaling. While fatty acid amide hydrolase (FAAH) is the principle AEA degrading enzyme, which breaks down AEA to generate ARA and ethanolamine, the primary 2-AG hydrolyzing enzyme is monoacylglycerol lipase (Mgll) that cleaves 2-AG to produce ARA and glycerol. Other eCB hydrolyzing enzymes include N-acylethanolamine-hydrolyzing acid amidase (NAAA) for AEA, and alpha/beta domain hydrolases 6 and 12 (ABHD6 and 12) for 2-AG hydrolysis. In addition, AEA and 2-AG can be oxidized by cyclooxygenase-2 (COX-2) leading to their degradation (Hermanson *et al.*, 2014).

Mgll is a 33 kDa serine hydrolase that is responsible for over 80 percent of 2-AG hydrolysis in the brain, making it the principle 2-AG hydrolyzing enzyme (Mulvihill and Normura, 2013; Chanda *et al.*, 2010). Given its central role in 2-AG hydrolysis, Mgll is localized in pre-synaptic axon terminals, with the highest expression in regions expressing eCBR1 (Dinh *et al.*, 2002). Recent work has revealed a significant role of Mgll in regulating lipid compositions to coordinate multiple lipid signaling pathways, particularly in linking the eCB system to the

eicosanoid system. Activation of Mgll not only reduces eCB signaling but also produces ARA, the precursor for pro-inflammatory eicosanoids. In fact, Mgll was recently identified as the major ARA-producing enzyme in the brain, a function previously thought to be exclusively carried out by phospholipase A2 (Normura *et al.*, 2011). ARA is metabolized by COX and lipoxygenases to produce eicosanoids, which are potent mediators of inflammation (Khanapure *et al.*, 2007).

The development of transgenic Mgll-null mouse models ($Mgll^{-/-}$) (Schlosburg *et al.*, 2010; Chanda *et al.*, 2010) and a highly selective Mgll activity inhibitor, JZL-184 (Long *et al.*, 2009) has greatly contributed to a better understanding of Mgll function. These studies demonstrate that genetic deletion of Mgll and/or inhibition of Mgll activity promotes anti-nociceptive, anti-inflammatory, anxiolytic and neuroprotective responses (Long *et al.*, 2009; Mulvihill and Normura, 2014). Mgll inhibition and/or deletion results in elevated 2-AG and reduced ARA, conferring a two-fold advantage in the brain. Increased 2-AG stimulates eCBR signaling to promote neurogenesis and neuroprotection, while decreased ARA levels further help to prevent neuroinflammation by reducing production of eicosanoids (Grabner *et al.*, 2016; Marsicano *et al.*, 2003; Panikashvili *et al.*, 2001), making Mgll a promising candidate against neuroinflammation/neurodegenerative disorders.

1.3. Alzheimer's Disease

Alzheimer's disease (AD), described for the first time in 1906 by the German psychiatrist Alois Alzheimer, is a progressive neurodegenerative disorder characterized by significant deficits in memory and cognition (Cummings, 2004; Lane *et al.*, 2017). It is the most common cause of

dementia that affects nearly 45 million people worldwide, with over half a million cases reported in Canada alone (Prince *et al.* 2015, Chambers *et al.* 2016). AD causes a significant socio-economic burden globally with costs of care for individuals with AD and other forms of dementia running into hundreds of billions of dollars (Prince *et al.*, 2015, Chambers *et al.*, 2016). This ever-increasing socio-economic impact of AD is the result of a rapidly-growing aging population and the lack of effective therapeutic approaches to treat AD.

1.3.1. Clinical Outcomes

AD is a fatal neurodegenerative disorder resulting in a gradual and progressive decline in memory and cognitive ability, accompanied by other serious behavioural abnormalities such as anxiety, depression and psychosis. AD-afflicted individuals usually experience difficulties in learning, problem-solving, verbal communication, as well as motor function (Caselli *et al.*, 2006; Lane *et al.*, 2017; Mega *et al.*, 1996; Scarmeas *et al.*, 2004). As AD progresses, patients lose routine life skills and require close supervision at all times (Forstl and Kurz, 1999).

1.3.2. Genetics and Risk Factors

AD occurs in two forms: a rare, early-onset familial form (FAD) and a late-onset sporadic form (SAD) that accounts for a majority (>95%) of AD cases (Marlatt *et al.*, 2009). FAD generally affects individuals with age ranging from 30 to 60 years and arises from autosomal-dominant mutations in genes encoding amyloid precursor protein (APP), presenilin-1 (PS1) or presenilin-2 (PS2), which result in overproduction of the toxic peptide amyloid beta (Aβ). SAD, the more widespread form of AD, usually afflicts individuals older than 65 years of age. Unlike FAD, the occurrence of SAD is governed by a complex interplay of environmental and inherited factors

(Tanzi, 2012; Lindsay *et al.*, 2002). While advanced age is the biggest environmental risk factor, presence of the ε4 allele of the apolipoprotein E (ApoE) gene is the strongest genetic risk factor for SAD (Bu, 2009; Lindsay *et al.*, 2002). In recent years, genome-wide association studies have identified genes involved in cholesterol and lipid metabolism pathways, inflammatory pathways, and endosomal vesicle cycling pathways, as additional genetic risk factors for AD (Van Cauwenberghe *et al.*, 2016; Karch and Goate, 2015). Besides these, gender, educational level, physical activity, hypertension, obesity and hyperlipidemia have also been implicated as risk factors by multiple studies (Lindsay *et al.*, 2002; Lange-Asschenfeldt and Kojda, 2008; Carroll *et al.*, 2010).

1.3.3. Hallmarks and Pathology

AD is characterized by two classic neuropathological hallmarks: Aβ plaques and neurofibrilliary tangles (NFTs). Aβ plaques are focal extracellular accumulations of the Aβ peptide (40-42 amino acids), derived from APP following its sequential cleavage by β- and γ-secretases. The resulting Aβ fibrils aggregate to form insoluble Aβ sheets that accumulate around neurons. Over time, these plaques associate with abnormal neuronal processes, termed dystrophic neurites, as well as activated microglia and astrocytes. The Aβ plaques occur mainly in the neocortex, with lesser known involvement of the temporal lobe, basal ganglia and the cerebellum (Wippold *et al.*, 2008; Serrano-Pozo *et al.*, 2011). NFTs are intraneuronal aggregations consisting of paired helical filaments of hyperphosphorylated tau. Tau is an important cytoskeletal protein that plays a key role in neuronal microtubule stabilization. However, hyperphosphorylation of tau occurs in AD, which results in tau aggregation and deregulation of the microtubule dynamics

(Metaxas and Kempf, 2016). NFTs, in contrast to Aβ plaques, typically appear in the entorhinal cortex and hippocampus (parts of the medial temporal lobe) and later spread to the neocortex (Metaxas and Kempf, 2016).

In addition to Aβ and NFTs, many other pathological changes including dystrophic neurites, axonopathy, cerebral amyloid angiopathy and the associated microglial and astrocytic activation are also commonly observed in AD. These changes are neurotoxic, which cause synaptic dysfunction and massive neuronal loss (Serrano-Pozo *et al.*, 2011; Selkoe, 2011; Lane *et al.*, 2017). Besides many microscopic alterations, AD also results in significant macroscopic atrophy particularly in the hippocampus, entorhinal cortex and amygdala (Jawahar, 2011; Bottino *et al.*, 2002).

1.3.4. Mouse models of AD

The advancement in our understanding of AD pathophysiology has mostly arisen from animal studies since many ethical, technical and practical limitations hamper assessment in humans and human tissues. Rodents, specifically mice, have been extensively used to generate transgenic models to better understand the pathophysiology of AD.

The earliest transgenic mouse models for AD involved the overexpression of human APP (hAPP) containing single or multiple FAD mutations. Several mouse models were developed using this approach, such as the Tg2576 mouse model carrying double mutations in hAPP, called the Swedish mutations ($hAPP_{Swe}$) (Hsiao *et al.*, 1996). These mice exhibited several AD-related neuropathological features such as elevated production of Aβ plaques, gliosis, dystrophic neurites as well as memory impairment (Hsiao *et al.*, 1996; Puzzo *et al.*, 2015). Following this,

efforts were made to generate double transgenic models by combining both APP and presenilin mutations to develop a more robust Aβ pathology. As expected, the APP/PS1 double transgenic mice displayed a more aggressive and earlier onset of Aβ pathology, as well as other pathological features such as early onset of abnormal long term potentiation (LTP) and memory impairments (Holcomb *et al.*, 1998, Arendash *et al.*, 2001; Hall and Roberson, 2012). In recent years, an even more aggressively progressing AD model, the 5xFAD, was generated by co-expressing five FAD-associated mutations including three APP and two PS1 mutations. These 5xFAD mice develop severe Aβ pathology quite rapidly, with intraneuronal Aβ accumulation occurring as early as 1.5 months of age and plaques and cognitive impairments becoming apparent at 4 months. Interesting, these mice are one of the only hAPP/PS1 models to develop AD-associated neuron loss (Oakley *et al.*, 2006; Jawahar *et al.*, 2012; Hall and Roberson, 2012; 5xFAD).

While most of the models described above successfully recapitulate a range of AD-related pathologies, they do not produce NFTs. To address this, a triple transgenic model, 3xTg, was developed (Oddo *et al.*, 2003b). Briefly, these mice were generated by co-injecting hAPP ($hAPP_{Swe}$) and hTau ($hTau_{P301L}$) transgenes, both under control of the Thy1.2 promoter, into the $PS1_{M146V}$ knock-in mouse embryos. The 3xTg mice develop a progressive AD neuropathology including Aβ plaques, NFTs, gliosis, impaired memory and cognition, as well as loss of LTP, all occurring in an age-dependent manner (Oddo *et al.*, 2003a; Oddo *et al.*, 2003b; Billings *et al.*, 2006). Additionally, the 3xTg mice develop significant impairments in adult neurogenesis, prior to the development of neuropathology and memory impairments (Hamilton *et al.*, 2010, 2015; Rodriguez *et al.*, 2008, 2009). An important advantage of the 3xTg mouse model is that these mice closely mimic human AD progression, especially in terms of the temporal and spatial

development of neuropathological features. As a result, this model is widely used for drug development and studying disease progression. Further, since the 3xTg mice exhibit perturbed neurogenesis and cognitive deficits long before the onset of pathological hallmarks (Hamilton *et al.*, 2010, 2015), they are particularly well-suited for examining how deregulated neurogenesis and its underlying molecular mechanisms predispose to AD during aging.

1.4. Neurogenesis and Alzheimer's Disease

Among the multiple pathological features observed in AD, the dilation of the lateral ventricles and significant hippocampal atrophy are of note since these alterations directly perturb the two major neurogenic niches in the brain (Perl, 2010). Given that the neurogenic niches are directly affected in AD, and AD-associated molecular players, namely ApoE, Tau, PS1, APP can regulate adult neurogenesis, it is reasonable to propose that AD-associated neuropathology impinges upon neurogenesis in the brain (Lazarov and Marr, 2011; Mu and Gage, 2011).

However, the relationship between neurogenesis and AD is contentious. While a majority of studies support the idea that AD is associated with reduced neurogenesis (Feng *et al.*, 2001; Haughey *et al.*, 2002; Zhang *et al.*, 2007; Wang *et al.*, 2004, Wen *et al.*, 2004), some studies show that neurogenesis is rather enhanced in AD (Lopez-Toledano and Shelanski, 2007; Yu *et al.*, 2009; Jin *et al.*, 2004a, 2004c). Notably, most studies that have reported increased hippocampal neurogenesis in AD only observed enhanced NPC proliferation or modest elevation in the expression of early neuronal markers, in the absence of concomitant increase in mature and functional neurons (Li *et al.*, 2008). In addition, many animal-based studies have shown that

increased neurogenesis is observed only at an early age (2-3 months) followed by sustained impaired neurogenesis at the middle and old ages (Mu and Gage, 2011; Gan *et al.*, 2008).

Similar findings have emerged from human studies as well. For instance, Jin and colleagues observed enhanced expression of only early neuronal markers such as DCX and PSA-NCAM in post-mortem AD brains (Jin *et al.*, 2004c). Another study showed that neurogenic changes associated with AD vary with the stage of the disease, and that increased NPC proliferation occurs in the absence of a concomitant increase in differentiated neurons (Perry *et al.*, 2012). Furthermore, Boekhoorn et al. showed that the AD-associated increase in NPC proliferation reflected enhanced gliogenesis and angiogenesis, but not neurogenesis (Boekhoorn *et al.*, 2006).

The disparity in these results can be attributed largely to the differences in technique, choice of animal model, age and history of the patients, stage of the disease, choice of immunohistochemical markers and PMD in tissue fixation. However, despite these discrepancies, it is clear that neurogenesis is altered in AD. Interestingly, most of the alterations in neurogenesis occur early in AD, prior to the appearance of other AD-associated neuropathological features which may secondarily hamper the neurogenic process (Lazarov and Marr, 2010; Mu and Gage, 2011). Recently, Hamilton et al. convincingly demonstrated that extensive neurogenic aberrations in the 3xTg AD mice occurred before the onset of Aβ plaques and NFTs deposition (Hamilton *et al.*, 2010, 2015). These findings suggest that this early occurrence of neurogenic impairments may potentially predispose to AD (Lazarov and Marr, 2010; Mu and Gage, 2011). As the disease progresses, the appearance of other neuropathological features may impair

neurogenesis further. Given the importance of adult neurogenesis in supporting hippocampal plasticity and cognition, impaired neurogenesis may mediate the cognitive decline in AD (Lazarov and Marr, 2010; Winner *et al.*, 2011).

1.5. Lipid Metabolism and Alzheimer's Disease

Increasing studies have implicated a role of lipid metabolism genes in AD pathogenesis (Hamilton *et al.*, 2015, 2018; Karch and Goate, 2015; Tanzi, 2012; Fraser *et al.*, 2010; Hussain *et al.*, 2013). Interesting, Alois Alzheimer himself reported atypical lipid changes as the third pathological hallmark of the disease, however, this was largely ignored until very recently (Alzheimer, 1907; Foley, 2010). Given the involvement of lipids in diverse brain functions, it is not surprising that aberrant lipid metabolism is associated with neurodegenerative diseases like AD.

Several lipids and lipid-related mechanisms have been implicated in AD pathogenesis. For instance, presence of the ε4 variant of ApoE (ApoE4) has been identified as the strongest genetic risk factor for SAD. In fact, studies have shown that individuals carrying two copies of ApoE4 have a 12-fold higher risk of developing AD than individuals who do not carry this allele (Liu and Zhang, 2014; Roses, 1996). ApoE is a major lipid transporter in the brain, which is involved in Aβ clearance. The low affinity of ApoE4 for Aβ results in impaired clearance causing Aβ accumulation. In addition, the presence of ApoE4 is associated with elevated cholesterol levels, which in turn contributes to AD pathology (Xu and Huang, 2006; Wong *et al.*, 2017). Cholesterol is abundantly present in the brain where it forms a vital component of cell membranes and myelin sheaths. However, increased cholesterol levels facilitate β-secretase

activity to promote Aβ production, as seen in AD. In addition, cholesterol enables conversion of soluble Aβ monomers to toxic oligomeric aggregates, accelerating AD pathogenesis (Liu and Zhang, 2014; Schneider *et al.*, 2006).

The eCB system has also been identified as a therapeutic target for AD in recent years (Pacher *et al.*, 2006). eCBR2 expression is markedly increased in post-mortem AD brains, especially on microglia surrounding senile plaques (Benito *et al.*, 2003; Ramirez *et al.*, 2005). Given the anti-inflammatory and neuroprotective role of eCBR2 signaling, increasing studies propose to activate eCBR2 as a promising therapeutic strategy against AD for attenuation of AD-associated neuroinflammation, as well as for modulating Aβ processing and improving cognition (Ramirez *et al.*, 2005; Benito *et al.*, 2003; Aso and Ferrer, 2016). Furthermore, Mgll has been identified as a promising therapeutic target against AD. An elegant study by Chen and colleagues successfully demonstrated the multiple beneficial effects of JZL-184 treatment (inhibition of Mgll activity) in the 5xFAD mice. These effects included reduced Aβ production and neuroinflammation, with a concurrent recovery in learning and memory deficits, as well as improved hippocampal synaptic function (Chen *et al.*, 2012).

Some recent work has also suggested a pathogenic role of aberrant fatty acid metabolism in AD. In a recent study, Hamilton et al. observed accumulations of lipid droplets in the neurogenic niche prior to the appearance of plaques and tangles in the 3xTg mice (Hamilton *et al.*, 2012). The same group later demonstrated that these triglyceride-enriched lipid droplets containing saturated, mono- and poly-unsaturated fatty acid (SFA, MUFA, PUFA) side chains,

suppress NSC activity early during AD and likely contribute to AD pathogenesis (Hamilton *et al.*, 2015).

In summary, there is compelling evidence that perturbed lipid metabolism and AD pathogenesis are intimately linked. However, the exact molecular and cellular mechanisms that drive these aberrations remain unknown. A better understanding of these processes is vital for the development of effective therapeutics against AD.

1.6. Epigenetic Regulation of Neurogenesis and Alzheimer's Disease: Role of the aPKC-CBP Pathway

Epigenetic modulation is a critical interface that integrates environmental signals into the determination of cell identity and function by altering gene expression without directly affecting the underlying DNA sequence (Jaenisch *et al.*, 2003; Zhang and Meaney, 2010). Epigenetic modulators have emerged as key regulators of neurogenesis, as well as other vital processes in the brain such as learning, cognition and memory formation (Ma *et al.*, 2010). There is now an increasing interest in understanding the contribution of these epigenetic mechanisms towards neurodegenerative disorders such as AD (Marques *et al*., 2011; Lardenoije *et al.*, 2015). Furthermore, since aging is characterized by widespread changes in the epigenetic landscape, it is plausible to hypothesize that dysregulated epigenetics during aging may contribute to AD predisposition.

In this regard, our recent work identifies the role of atypical protein kinase C (aPKC) mediated Ser436 phosphorylation in CREB-binding protein (CBP), a histone acetyltransferase

(HAT), as an important mechanism that sustains hippocampal neurogenesis and memory during normal aging (Gouveia *et al.*, 2016). In this study, our group demonstrated that CBPS436A knock-in (KI) mice, which lack a functional aPKC-CBP pathway due to replacement of serine (S) 436 with alanine (A) in CBP, display impaired hippocampal neuronal differentiation and hippocampus-associated memory at the age of 6 months but not 3 months (Gouveia *et al.*, 2016). Furthermore, other studies from our lab have demonstrated that metformin, an FDA-approved anti-diabetic drug, activates the aPKC-CBP pathway to promote SVZ-NPC neuronal differentiation in culture and also improve hippocampus-associated cognition and memory *in vivo* (Wang *et al.*, 2012; Fatt *et al.*, 2015). Interestingly, the effects of metformin on neurodegeneration-related cognitive decline reveal conflicting results in the clinical setting, likely due to multiple off-target effects of metformin (Ng *et al.*, 2014; Moore *et al.*, 2013). Therefore, identifying the exact molecular targets through which metformin acts to promote cognition is vital.

To this end, we conducted an RNA-seq analysis using differentiating WT and CBPS436A NPCs cultured in the presence of metformin to identify the direct targets of the aPKC-CBP pathway. Of the 46 genes that were dysregulated in CBPS436A NPCs, we singled out an upregulated gene, Mgll, as the major mediator the aPKC-CBP pathway (experiments done by other lab members). To further confirm our RNA-seq data, we assessed Mgll mRNA and protein levels in CBPS436A SVZ NPCs and hippocampal tissue respectively (**Figure 1 A, C**), and observed that Mgll is aberrantly upregulated in the CBPS436A NPCs and hippocampal tissue. Using a ChIP-qPCR analysis we further showed enhanced CBP binding at the Mgll promoter in the CBPS436A NPCs, suggesting that CBP directly regulates Mgll expression.

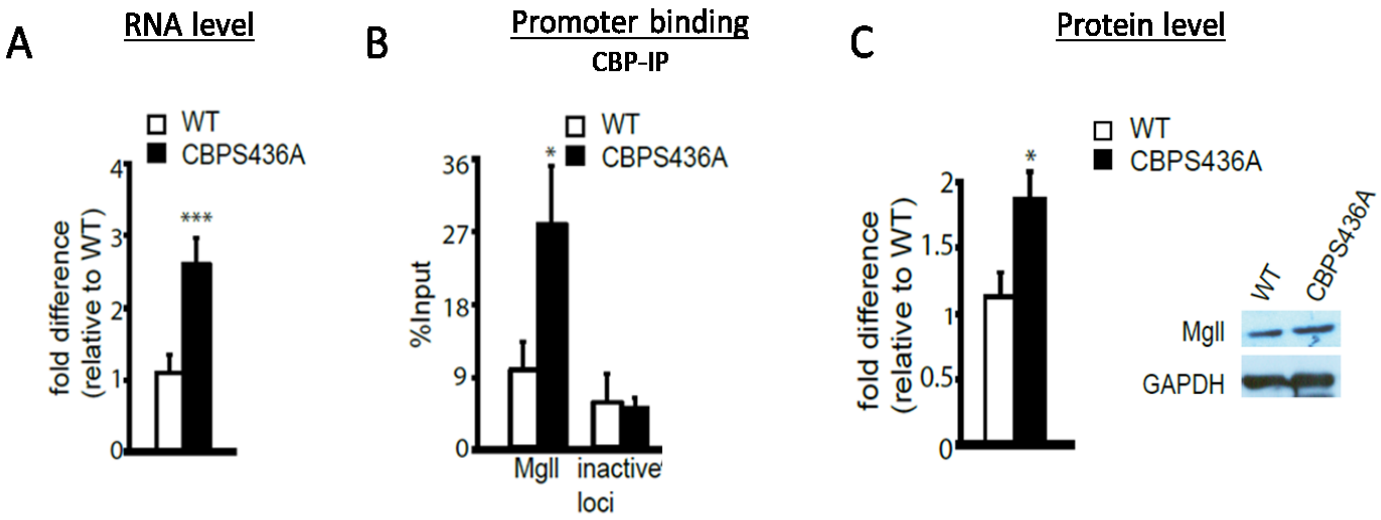

Figure 1. Mgll is aberrantly upregulated in CBPS436A mice. (A) Quantitative PCR (qPCR) for Mgll mRNA from differentiating WT and CBPS436A NPCs in the presence of metformin. *** $p < 0.001$ (n=4). **(B)** ChIP-qPCR analysis for CBP binding at Mgll promoter in differentiating WT and CBPS436A NPCs in the presence of metformin. * $p < 0.05$ (n=3). (C) Western blot analysis for Mgll protein levels in 6-month old CBPS436A hippocampal tissues. *$p < 0.05$ (n=3).

Intriguingly, previous studies have reported reduced PKC levels and/or activity in the AD brain (Masliah *et al.*, 1991; Moore *et al.*, 1998; Etcheberrigaray *et al.*, 2004; Tan *et al.*, 2010; Talman *et al.*, 2016). In addition, Mgll was recently identified as a therapeutic target against AD (Chen *et al.*, 2012). However, what causes dysregulation of Mgll in AD and how that potentially contributes to cognitive dysfunction remains unknown.

Therefore, based on our recent findings (Gouveia *et al.*, 2016; **Figure 1**), we propose that the aPKC-CBP pathway directly regulates Mgll expression to control 2-AG versus ARA signaling to determine NPC fate in the normal and AD brain.

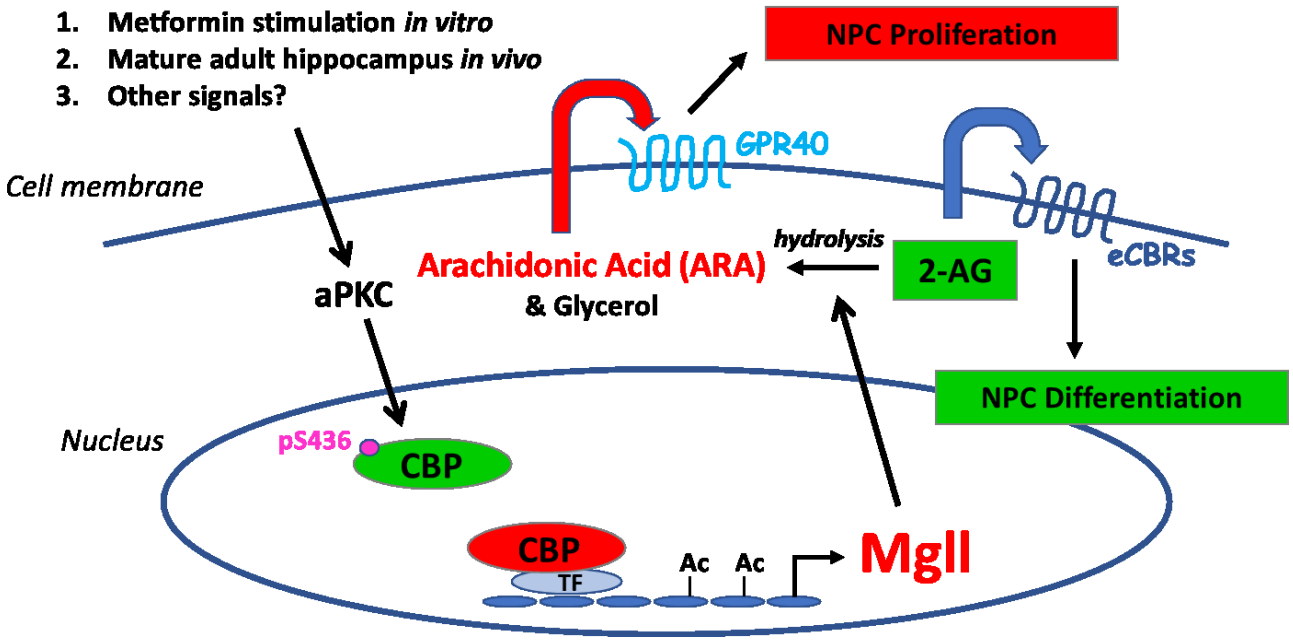

Diagram 1: Schematic overview of the study

2. Hypothesis and Objectives

2.1. Hypothesis

We hypothesize that activation of the aPKC-CBP pathway directly represses Mgll expression to modulate NPC proliferation and differentiation by altering 2-AG versus ARA levels; and that attenuation of the aPKC-CBP pathway in AD NPCs increases Mgll levels and impairs NPC function, consequently predisposing to AD.

2.2. Objectives

Objective 1: Investigate the role of Mgll in transducing the aPKC-CBP pathway to modulate NPC proliferation and differentiation

Objective 2: Examine whether and how attenuation of the aPKC-CBP mediated Mgll repression perturbs NPC function in the 3xTg AD NPCs

3. Materials and Methods

3.1. Animals

All animal use was approved by the Animal Care Committees of the University of Ottawa in accordance with the Canadian Council of Animal Care policies. Transgenic mouse lines CBPS436A and 3xTg were maintained on a 12 h light/dark cycle with food and water available *ad libitum*. The transgenic CBPS436A mouse line was obtained from the laboratory of Dr. Fredric Wondisford (Rutgers-Robert Wood Johnson Medical School, New Brunswick, NJ, USA). Heterozygous CBPS436A were bred to produce WT and homozygous CBPS436A animals for the experiments. The 3xTg mice (homozygous for $PS1_{M146V}$, APP_{Swe} and Tau_{P301L} mutations on a hybrid C57BL6/129S genetic background) and non-transgenic, Non-Tg mice (C57BL6/129S), originally generated at the laboratory of Dr. Frank M LaFerla (University of California, Irvine, USA), were purchased from the Jackson Laboratory. The generation of the transgenic CBPS436A and 3xTg lines has been described previously (Zhou *et al.*, 2004; Oddo *et al.*, 2003).

3.2. NIH3T3 Cell Culture

NIH3T3 cells, gifted by Dr. Xiaohui Zha (Ottawa Hospital Research Institute, Ottawa, Canada), were cultured in high glucose Dulbecco's Modified Eagle's Medium (DMEM) (Wisent Bioproducts, 319-005-CL) containing 10% fetal bovine serum (FBS) (Life Technologies, 12484010) and 1% penicillin-streptomycin (Thermo Fisher, 15140122). The cells were maintained in a humidified incubator at 37°C with 5% CO_2 and passaged every three days. For transfection, the

cells were seeded in 6-well culture plates at 500,000 cells per well. Following overnight incubation, cells were transfected with Mgll shRNA 1 (2.5 µg), Mgll shRNA 2 (2.5 µg), Mgll shRNAs 1 and 2 (1.25 µg for each), or a non-specific scrambled (Scr) shRNA (2.5 µg) (Appendix, Table 1), mixed with 7.5 µL of TransIT-X2® Dynamic Delivery System (Mirius, MIR6003) in Opti-MEM™ (Thermo Fisher, 31985062) per well. Cells were harvested 48 hours later, and the knockdown efficiency was assessed using a western blot.

3.3. Adult Neurosphere Culture

Subventricular zone (SVZ) tissues were microdissected from the subependyma of lateral ventricles of six to eight week old mice (WT, CBPS436A, Non-Tg and 3xTg). The collected tissues were digested in 5-10 mL enzyme mix (Appendix, Table 2) for 40 minutes at 37°C while mixing on a HulaMixer™ Sample Mixer. Digestion was stopped using a sterilized trypsin inhibitor (0.67 mg/mL) (Sigma-Aldrich, T2011-500) prepared in serum-free medium (SFM) (Appendix, Table 2). The tissues were mechanically dissociated into single cell suspensions by passing through P1000 and P200 pipettes and cells were collected by centrifuging twice at 390g for 5 minutes. The cell pellet was resuspended in supplemented SFM (SFM+EFHB) containing 20 ng/mL epidermal growth factor (EGF; E) (Sigma-Aldrich, E9644), 20 ng/mL basic fibroblast growth factor (bFGF; F) (PeproTech, 100-18B), 2 µg/mL heparin (H) (Sigma-Aldrich, H3149-100KU) and 1x B-27™ supplement (B) (Thermo Fisher Scientific, 17504-044). Live cells were counted using trypan blue (Thermo Fisher Scientific, 15250061), plated at 10 cells/µL in 6-well plates, and cultured for seven days *in vitro* (DIV) without disturbance in a humidified incubator at 37°C with 5% CO_2 to allow

neurosphere (NS) formation. Free-floating primary NS were collected and centrifuged at 390g for 5 minutes. The supernatant was discarded, and the cell pellets were resuspended and dissociated into single-cell suspensions by triturating in supplemented SFM. The cells were filtered through a cell strainer (40 µm pore size), counted, and seeded at 2 cells/µL in 6 well plates to initiate secondary NS formation. Six days later, the secondary NS or second passage (P2) NPCs were collected and passaged until the fifth passage (P5) or used for further experiments as described below.

The remaining P2 WT, CBPS436A, Non-Tg and 3xTg NPCs and P5 WT and CBPS436A NPCs were pelleted and washed with 1x PBS. Excess PBS was discarded, and the cells were snap-frozen in liquid nitrogen followed by storage at -80°C until required.

3.4. NPC Differentiation

WT and CBPS436A P2 NPCs were plated on poly-L-ornithine (PLO) (Sigma-Aldrich, P4957, 15% prepared in sterile water) and laminin (Thermo Fisher Scientific, CB40232, 0.05% prepared in sterile water) coated 6-well plates at 1,000,000 cells per well in neural differentiation medium: SFM containing 10% FBS, supplemented with 1 µM metformin (Sigma-Aldrich, PHR1084-500MG). The differentiating NPCs were harvested seven days upon differentiation for western blot analysis.

3.5. NPC Transfection and Conditioned Medium Treatment

WT, CBPS436A, Non-Tg and 3xTg P2 or P5 NPCs were plated on PLO-laminin coated coverslips at 100,000 cells per well in 24-well plates, in supplemented SFM (SFM+EFHB). Following overnight incubation, each well was transfected with either 0.4 µg Mgll shRNA 1 and 2 (0.2 µg for each) or 0.4 µg phosphomimic CBPS436D plasmid (Wang *et al.*, 2012) together with 0.2 µg of a CAG-eGFP (eGFP) plasmid (Wang *et al.*, 2012), mixed with 1.8 µL of TransIT-X2® Dynamic Delivery System (Mirius, MIR6003) in Opti-MEM™ (Thermo Fisher, 31985062). In these experiments, non-specific Scramble shRNA (mentioned earlier) and pcDNA3.1 empty vector (Wang *et al.*, 2012) were transfected in separate wells as controls for Mgll shRNA and CBPS436D plasmid, respectively. 24 hours following transfection, the medium was switched to neural differentiation medium (SFM+10% FBS), supplemented with 1 µM metformin. Conditioned medium (CM) from differentiating WT and CBPS436A NPCs was collected seven days upon differentiation, centrifuged at 16200g for 10 minutes, and stored at -20°C for later use, while transfected cells were assessed using immunocytochemistry as described below.

Another set of WT and CBPS436A P2 NPCs were plated on PLO-laminin coated coverslips at 100,000 cells per well in 24-well plates, in SFM+EFHB. Following overnight incubation, the medium was changed to neural differentiation medium containing 50% of the previously collected CM and supplemented with 1 µM metformin. The NPCs were assessed seven days later using immunocytochemistry as described below.

3.6. Neurosphere Size Assessment and GPR40 Antagonist Treatment

DC 260126 (Tocris, 5357-10), a GPR40 antagonist was prepared in dimethyl sulfoxide (DMSO) (Sigma-Aldrich, D2650) as a 1 mM stock and stored at -20°C. 3xTg and Non-Tg P2, and WT and CBPS436A P5 NPCs were treated with 100 nM DC 260126 or 0.01% DMSO (control) at time of plating (2 cells/ul in 6-well plates), and neurospheres were imaged and assessed six days later as described below.

3.7. Drug Treatment in Cultured NPCs

Mgll inhibitor, JZL-184 (Cayman Chemical, 13158-5) and eCBR1 and eCBR2 agonists, ACEA (Arachidonyl-2'-chloroethylamide) (Cayman Chemical, 91054) and JWH-133 (Tocris, 1343-10) respectively, were prepared in DMSO as a 1 mM stock, while metformin (Sigma-Aldrich, D150959-5G) was prepared as a 0.5 mM stock in sterilized water. All reagents were stored at -20°C until required.

3xTg and Non-Tg P2 NPCs were plated on PLO-laminin coated coverslips in a 24-well plate at 100,000 cells per well and cultured in SFM containing 10% FBS. The media was supplemented with 500 nM metformin, 1 μM JZL-184, 1 μM ACEA or 1 μM JWH-133. Water treatment or 0.1% DMSO were used as control groups. The differentiating NPCs were cultured for seven days and assessed by immunocytochemistry as described below.

3.8. Immunocytochemistry

Cells growing on PLO-laminin coated glass coverslips were retrieved from the incubator. The medium was discarded, and the cells were washed with 1x PBS for 5 minutes followed by a 10-minute fixation in 4% PFA. Following three 5-minute 1x PBS washes, the coverslips were removed from the wells and blocked/permeabilized for one hour at room temperature in 10% normal goat serum (NGS) (Thermo Fisher Scientific, 16050122) with 0.3% Triton™ X-100 prepared in 1x PBS.

The coverslips were then incubated with the primary antibody prepared in 10% NGS with 0.3% Triton™ X-100 in 1x PBS, at 4°C overnight. The antibodies used were: chicken anti-GFP (1:2000, Abcam, ab13970) and/or mouse anti-βIII tubulin (1:500, Biolegend, 801201). Following overnight antibody incubation, the coverslips were washed three times for 5 minutes each with 1x PBS, and then incubated with Alexa Fluor-conjugated secondary antibody: goat anti-chicken Alexa Fluor 488 (1:500, Thermo Fisher Scientific, A11039) and donkey anti-mouse Alexa Fluor 555 (1:500, Thermo Fisher Scientific, A31572), diluted in 0.3% Triton™ X-100 solution in 1x PBS for one hour at room temperature. Immediately after secondary antibody incubation, the coverslips were counterstained with Hoechst 33342 stain (Cell Signalling Technology, 4082S) at 1 µg/mL in 1x PBS for 5 minutes followed by three 5-minute washes in 1x PBS. The coverslips were mounted on clean glass slides with PermaFluor™ solution and imaged once dry.

3.9. JZL-184 and 5-Bromo-2'-deoxyuridine (BrdU) Injections

JZL-184 (Cayman Chemical, 13158-50) was prepared in DMSO at 40 mg/mL and stored at -20°C. Dissolved JZL-184 was mixed with 2.5% Tween-80 in 1x PBS and administered the same day. 6-month-old WT and CBPS436A mice received a daily intraperitoneal (i.p.) injection of 8 mg/kg JZL-184 or saline containing 2.5% Tween-80 and 2% DMSO as a control for 14 days. To label dividing cells, the mice also received two i.p. injections of BrdU (Sigma-Aldrich, B9285-1G, 100 mg/kg), 4 hours apart, for three consecutive days, after an initial two days of treatment with JZL-184 alone.

3.10. Tissue Preparation

Following 14 days of JZL-184 injections, mice were anesthetized with 0.1 mL sodium pentobarbital (65 mg/mL, i.p.). Mice were then transcardially perfused with 70 mL (7 mL/minute for 10 minutes) of 4°C 1x PBS followed by 70 mL (7 mL/minute for 10 minutes) of 4°C 4% paraformaldehyde (PFA) (Sigma-Aldrich, 158127) in 1x PBS. The brains were extracted and post-fixed in 4% PFA overnight at 4°C, followed by storage in 30% sucrose solution containing 0.1% sodium azide (Fisher Scientific, 19038) for at least 48 hours. Samples were covered in optimal cutting temperature solution (VWR, 95057-838) and flash frozen on dry ice. Serial 20 µm hippocampal sections were obtained using a cryostat (Leica Biosystems, CM1850) and sequentially mounted on 10 glass slides, to encompass the entire hippocampus. Sections were stored at -80°C until required.

3.11. Immunohistochemistry

The tissue sections were retrieved from -80°C and thawed at 37°C for 10 minutes. The sections were washed twice with 1x PBS followed by a 15-minute fixation with 4% PFA. Following three 5-minute washes, the sections were treated with 1 N HCl at 45°C for 1 hour and then extensively washed with 1x PBS. The sections were then blocked/permeabilized for at least one hour at room temperature in 10% normal horse serum (NHS) (Thermo Fisher Scientific, 16050122) with 0.3% Triton™ X-100 (Fisher Scientific BP151-100) prepared in 1x PBS.

The brain sections were sequentially incubated with the primary antibody prepared in 10% NHS with 0.3% Triton™ X-100 in 1x PBS, at 4°C overnight. The antibodies used were: rat anti-BrdU (1:200, AbD Serotec, OBTOO30G) and mouse anti-NeuN (1:500, Millipore, MAB377). Following overnight incubation for each primary antibody, the sections were washed three times for 5 minutes each with 1x PBS, before addition of an Alexa Fluor-conjugated secondary antibody: donkey anti-rat Alexa Fluor 488 (1:500, Thermo Fisher Scientific, A21208) or goat anti-mouse Alexa Fluor 647 (1:500, Thermo Fisher Scientific, A-21235), diluted in 0.3% Triton™ X-100 solution in 1x PBS for one hour. After last secondary antibody incubation, the sections were washed three times for 5 minutes each in 1x PBS and mounted using PermaFluor™ solution (Thermo Fisher Scientific, TA-030-FM). The slides were assessed once dry.

3.12. Imaging and quantification

P2 and P5 neurospheres were imaged at 5x magnification, with Zeiss Axiovert 200M inverted microscope using Zeiss Axiovision software. Eight to ten images were randomly taken

per treatment group and neurosphere diameters were measured using FIJI software. On average, 300-400 neurospheres were assessed per condition.

Fluorescent images were taken on a Zeiss Axioplan 2 fluorescent microscope with Z-axis capability, using Zeiss Axiovision software. For *in vitro* transfection experiments, 100-200 GFP positive cells were quantified per condition. For all other *in vitro* experiments eight to ten images were taken randomly at 20x magnification, and on average 800-1000 cells were quantified per condition. Cell counts were done blinded to experimental groups, using FIJI software.

In vivo quantification was performed as described previously (Gouveia *et al.*, 2016). Briefly, every tenth section throughout the septotemporal axis of the hippocampus (-1.3 mm to -3.70 mm relative to bregma referring to the rostral-caudal coordinates) was analyzed. 15-20 images were captured per section in the Z-axis at 1 µm apart and processed as an optical stack of 10-15 slices for quantification. Every BrdU positive cell within the dentate gyrus region including the SGZ, granular cell layer and hilus was exhaustively quantified. On average, 100-150 BrdU positive cells were quantified per slide.

3.13. Western blot

Cultured cells or frozen cell pellets (thawed on ice) were lysed in cold lysis buffer (Appendix, Table 3) containing 1 mM sodium orthovanadate (Sigma-Aldrich S6508-10G), 20 mM sodium fluoride (Fisher Scientific, AC201295000), 1mM PMSF (Sigma-Aldrich, P7626-5G), 10 µg/mL aprotinin (Fisher Scientific, PI78432) and 10 µg/mL leupeptin (Fisher Scientific, PI78436). The lysates were homogenized by trituration, and sonicated (three 5-second pulses with 1 minute

intervals), followed by centrifugation at 16200g for 15 minutes at 4°C. Total protein amount in the supernatant for each sample was quantified using Pierce BCA Protein Assay Kit (Thermo Fisher Scientific, 23227) according to manufacturer's instructions. The samples were stored at -80°C until use.

Protein samples (20-30 µg) were mixed with 5x sample buffer (Appendix, Table 3), boiled at 95°C for 5 minutes, and resolved on a 12% SDS-polyacrylamide gel in running buffer (Appendix, Table 3). The proteins were transferred from the gel to a nitrocellulose blotting membrane (GE Healthcare Life Sciences, 10600009) in transfer buffer (Appendix, Table 3) for one hour at 100 V. After a quick rinse in 1x TBS-T (Appendix, Table 3), the membrane was blocked in 3% bovine serum albumin (BSA) (New England Biolabs, 9998S) solution prepared in 1x TBS-T for one hour. Primary antibodies solutions were prepared in 3% BSA in 1x TBS-T for rabbit anti-Mgll (1:1000, Abcam, ab24701), rabbit anti-pT410/403-aPKCζ/ι (1:500, Cell Signalling Technology, 9378S), rabbit anti-acetyl H2B (1:1000, Abcam, ab40886), mouse anti-aPKCζ/ι (1:1000, BD Biosciences, 610175), mouse anti-H2B (1:40,000, Abcam, ab52484) or mouse anti-GAPDH (1:50,000, Abcam, ab8245) antibodies. The membranes were incubated with the primary antibody solution overnight at 4°C followed by five 5-minute washes in 1x TBS-T next day. The membranes were incubated with an HRP-conjugated secondary antibody: goat anti-rabbit or anti-mouse (1:3000, Cell Signalling Technologies, 7074 and 7076, respectively) for one hour at room temperature. Following five 5-minute washes in 1x TBS-T, the membranes were treated with Pierce ECL Western Blotting Substrate (Thermo Fisher Scientific, PI32209) for one minute. Exposures between 5 seconds and 20 minutes were taken on HyBlot CL films (Denville Scientific, DV-E3018) and developed using an automatic X-Ray Film processor.

3.14. Statistical Analysis

All data analysis was conducted using GraphPad Prism 6 software. Statistical analyses were performed using either a two-tailed Student's t-test, one-way ANOVA with Dunnett's post-hoc test or two-way ANOVA with Tukey's post-hoc test. All values are expressed as mean ± standard error of the mean (SEM). For all experiments, differences with p-value < 0.05 were considered statistically significant.

4. Results

4.1. Mgll expression is elevated in differentiating CBPS436A NPCs

Our preliminary data indicates that SVZ-derived differentiating CBPS436A NPCs from secondary neurospheres (passage 2, P2) exhibit elevated Mgll mRNA levels as compared to their WT littermates in the presence of metformin (**Figure 1 A**). To assess if these increased Mgll mRNA levels corresponded with enhanced Mgll protein expression, I examined Mgll protein levels in differentiating CBPS436A and WT P2 SVZ NPCs. The results showed a marked elevation in Mgll protein expression in the CBPS436A NPCs relative to WT NPCs in the presence of metformin (**Figure 2**), suggesting that constitutive inactivation of the aPKC-CBP pathway is associated with increased Mgll protein levels.

To assess whether increased Mgll levels in the CBPS436A P2 NPCs were associated with enhanced histone acetylation, I examined histone H2B acetylation at lysine residue 5 (H2BK5), a major site acetylated by CBP (Valor *et al.*, 2011), in the differentiating NPCs. I observed a significant increase in the amount of acetylated H2BK5 in the differentiating CBPS436A NPCs relative to WT NPCs, suggesting that enhanced histone acetylation by CBPS436A contributes to increased Mgll gene expression in these NPCs (**Figure 3**).

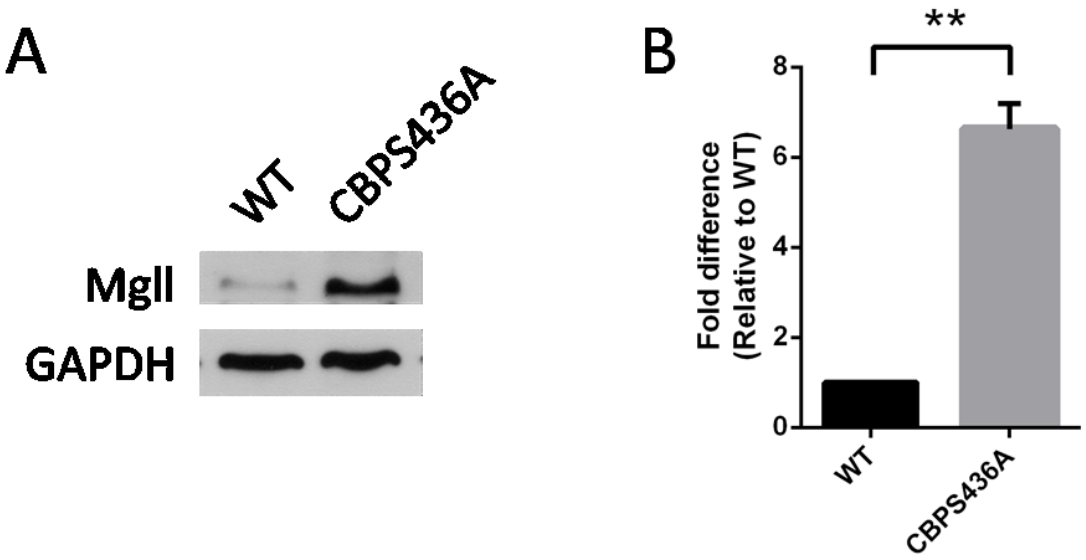

Figure 2: CBPS436A NPCs exhibit elevated Mgll expression. (A) Representative western blot images of whole protein lysates from differentiating (7 DIV, in the presence of 1 µM metformin) WT and CBPS436A P2 NPCs probed for Mgll, with GAPDH as a loading control. **(B)** Quantitative analysis of Mgll protein expression in differentiating WT and CBPS436A P2 NPCs, normalized to GAPDH. Student's t-test was performed for n = 4 samples. ** $p < 0.01$.

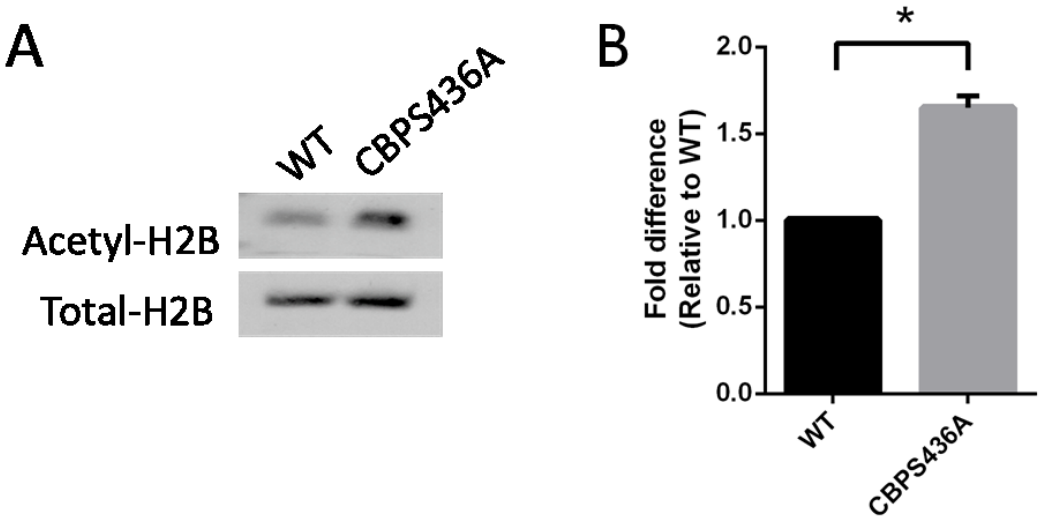

Figure 3: CBPS436A NPCs exhibit elevated acetyl-H2B levels. (A) Representative western blot images of whole protein lysates from differentiating (7 DIV, in the presence of 1 µM metformin) WT and CBPS436A P2 NPCs probed for acetyl-H2BK5, and re-probed for total-H2B as a loading control. **(B)** Quantitative analysis of acetyl-H2BK5 expression in differentiating WT and CBPS436A P2 NPCs, normalized to total-H2B. Student's t-test was performed for n = 3 samples. * $p < 0.05$.

4.2. Genetic knockdown of Mgll rescues NPC differentiation deficits in CBPS436A NPCs *in vitro*

Previous studies have demonstrated that CBPS436A NPCs, which lack a functional aPKC-CBP pathway, do not respond to metformin to promote NPC differentiation, and therefore exhibit significant neuronal differentiation deficits in the presence of metformin (Fatt *et al.*, 2015). Given that these neuronal differentiation deficits occur concurrently with elevated Mgll levels in the CBPS436A P2 NPCs (**Figure 2**), I asked if elevated Mgll expression was responsible for these differentiation deficits. To examine this, we designed two Mgll shRNAs (Mgll shRNA 1, Mgll shRNA 2), each targeting a different region of the Mgll transcript, and a non-specific Scramble (Scr) shRNA. I first assessed the knockdown efficiency of these shRNAs using NIH3T3 cells, a mouse embryo fibroblast cell line. I found that the combination of Mgll shRNA 1 and 2 consistently and efficiently reduced Mgll protein levels, and thus chose it for further analyses (**Figure 4**).

To assess the role of Mgll in mediating the aPKC-CBP pathway to regulate NPC neuronal differentiation, I transfected WT and CBPS436A P2 SVZ NPCs with Mgll or Scr shRNAs, together with a CAG-eGFP plasmid as a marker for transfection efficiency. 24 hours following transfection, these NPCs were directed to differentiate in the presence of metformin (1 μM) for seven days. Neuronal differentiation was assessed by immunocytochemistry for GFP and βIII tubulin, a newborn neuron marker. Consistent with our previous findings, I observed that Scr shRNA-transfected CBPS436A P2 NPCs did not respond to metformin treatment, exhibiting a significant neuronal differentiation deficit measured by a reduced percentage of βIII tubulin$^+$ newborn neurons produced from total GFP$^+$ transfected CBPS436A NPCs as compared to the Scr shRNA-

transfected WT NPCs. Knockdown of Mgll by Mgll shRNA transfection rescued this differentiation deficit in the CBPS436A P2 NPCs, measured by a significant increase in the percentage of βIII tubulin^{+} neurons as compared to the Scr shRNA-transfected CBPS436A P2 NPCs (**Figure 5 A, B**). Interestingly, the WT P2 NPCs transfected with Mgll shRNAs also produced a higher percentage of newborn neurons, as compared to their Scr shRNA controls (**Figure 5 A, B**). These results support that Mgll knockdown rescues CBPS436A P2 NPC neuronal differentiation deficits in a cell-intrinsic manner.

Intriguingly, quantification of the percentage of βIII tubulin^{+}/GFP^{-} neurons (generated from non-transfected NPCs) out of total live cells in the same set of experiments, revealed a similar rescue of differentiation deficit upon Mgll knockdown (**Figure 5 C, D**). These results indicate that Mgll knockdown additionally acts in a cell-extrinsic manner to promote NPC neuronal differentiation.

To further confirm the cell-extrinsic effect, I collected conditioned media (CM) from differentiating WT and CBPS436A P2 NPCs transfected with Scr or Mgll shRNAs and treated a fresh set of P2 NPCs with this CM for 7 DIV in the presence of metformin (1 μM), without direct Mgll knockdown. Immunostaining analysis of the percentage of βIII tubulin^{+} neurons generated from the CM-treated NPCs showed a consistent neuronal differentiation deficit in the CBPS436A NPCs as compared to the WT NPCs, both treated with CM from Scr shRNA transfected NPCs (**Figure 5 E, F**). This differentiation defect in the CBPS436A P2 NPCs was rescued upon treatment with CM from Mgll-shRNA transfected CBPS436A NPCs (**Figure 5 E, F**), in a similar manner as the

CBPS436A P2 NPCs that were directly transfected with Mgll shRNA. These results confirm the cell-extrinsic effects of Mgll knockdown in rescuing neuronal differentiation deficits.

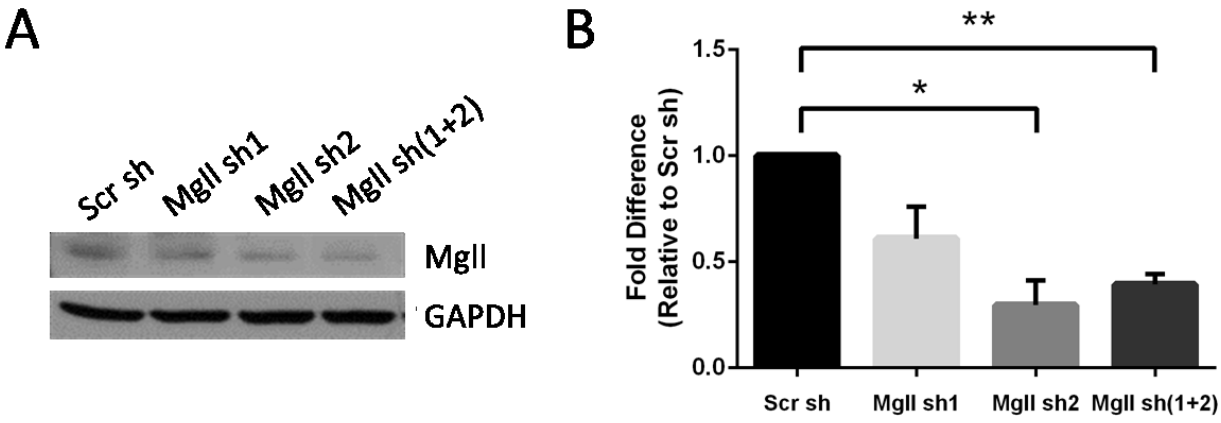

Figure 4: Efficiency of shRNA-mediated Mgll knockdown. (A) Representative western blot images of total protein lysates from NIH3T3 cells transfected with Mgll shRNAs and a Scr shRNA, probed for Mgll and GAPDH (a loading control). **(B)** Quantitative analysis of Mgll expression in NIH3T3 cells 48h after shRNA transfection, normalized to GAPDH. Data from 3 independent experiments was analyzed using one-way ANOVA ($F_{(3, 8)} = 10.09$, $P = 0.0043$) with Dunnett's post-hoc test. * $p < 0.05$, ** $p < 0.01$. (Scr sh: Scramble shRNA; Mgll sh1: Mgll shRNA 1; Mgll sh2: Mgll shRNA 2).

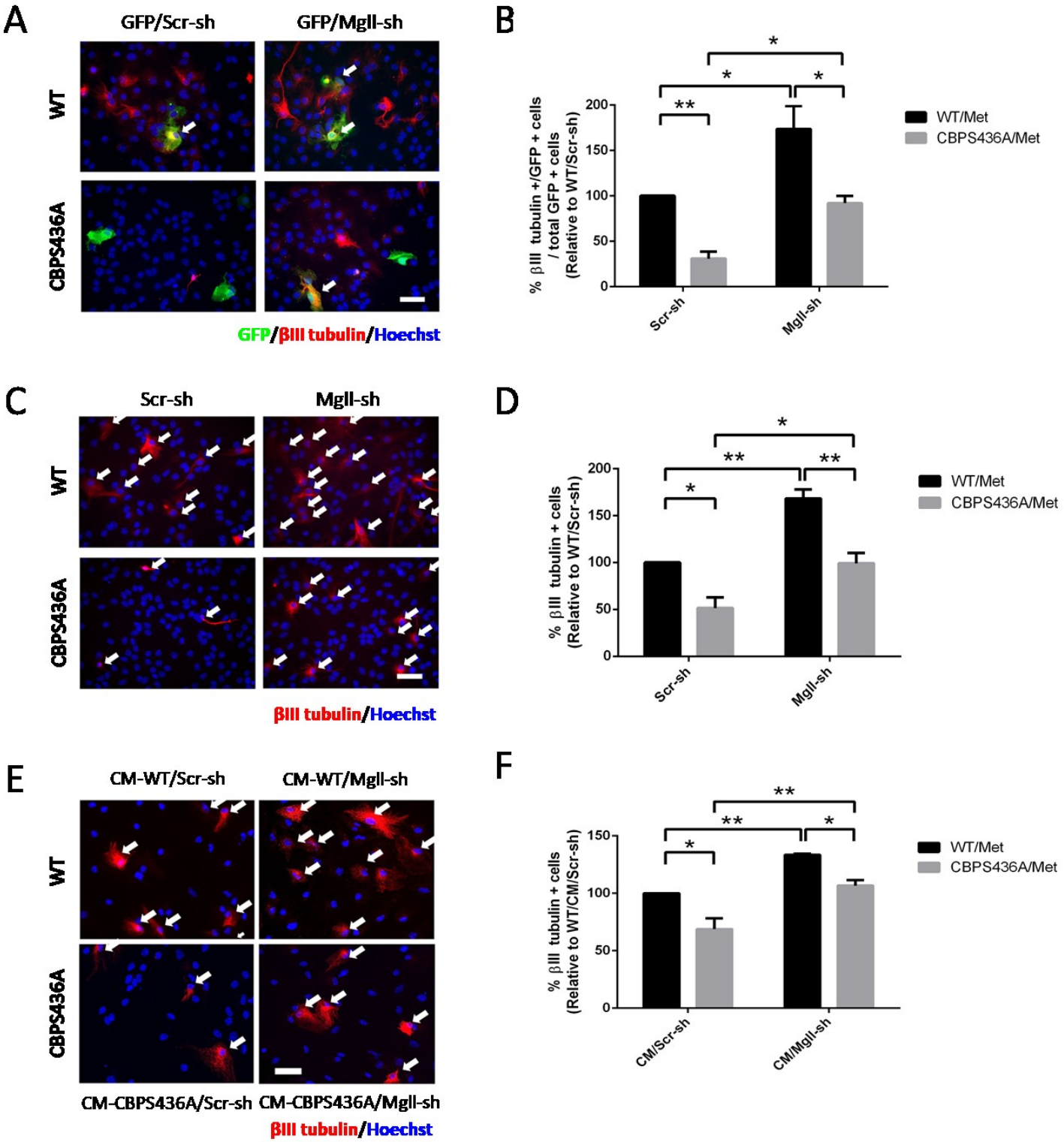
A
GFP/Scr-sh
GFP/Mgll-sh
WT
CBPS436A
GFP/βIII tubulin/Hoechst
B
% βIII tubulin +/GFP + cells / total GFP + cells (Relative to WT/Scr-sh)
200
150
100
50
0
*
*
*
**
Scr-sh
Mgll-sh
WT/Met
CBPS436A/Met
C
Scr-sh
Mgll-sh
WT
CBPS436A
βIII tubulin/Hoechst
D
% βIII tubulin + cells (Relative to WT/Scr-sh)
200
150
100
50
0
*
**
*
**
Scr-sh
Mgll-sh
WT/Met
CBPS436A/Met
E
CM-WT/Scr-sh
CM-WT/Mgll-sh
WT
CBPS436A
CM-CBPS436A/Scr-sh
CM-CBPS436A/Mgll-sh
βIII tubulin/Hoechst
F
% βIII tubulin + cells (Relative to WT/CM/Scr-sh)
150
100
50
0
**
**
*
*
CM/Scr-sh
CM/Mgll-sh
WT/Met
CBPS436A/Met

Figure 5: Mgll knockdown rescues neuronal differentiation deficits of CBPS436A NPCs in cell intrinsic and cell extrinsic manners. (A, B) Immunofluorescent images and quantitative analysis of the percentage of βIII tubulin^{+}/GFP^{+} co-labeled neurons out of total GFP^{+} cells from differentiating WT and CBPS436A P2 NPCs following transfection with Scr or Mgll shRNAs, together with eGFP plasmid. Data was analyzed by two-way ANOVA (Genotype x treatment $F_{(1,8)}$ = 0.0642, p = 0.8064; Treatment $F_{(1,8)}$ = 21.56, p = 0.0017; Genotype $F_{(1,8)}$ = 28.02, p = 0.0007) with Tukey's post-hoc test for n = 3 independent experiments. **(C, D)** Immunofluorescent images and quantitative analysis of the percentage of βIII tubulin^{+}/ GFP^{-} cells out of total differentiating WT and CBPS436A P2 NPCs following transfection with Scr or Mgll shRNAs, together with eGFP plasmid. Data was analyzed by two-way ANOVA (Genotype x treatment $F_{(1,12)}$ = 1.230, p = 0.2891; Treatment $F_{(1,12)}$ = 39.05, p < 0.0001 ; Genotype $F_{(1,12)}$ = 40.37, p < 0.0001) with Tukey's post-hoc test for n = 4 independent experiments. **(E, F)** Immunofluorescent images and quantitative analysis of the percentage of βIII tubulin^{+} neurons out of total live WT and CBPS436A P2 NPCs treated with 50% conditioned media (CM) from differentiating P2 NPCs transfected with Scr or Mgll shRNAs. Data was analyzed by two-way ANOVA (Genotype x treatment $F_{(1,8)}$ = 0.1839, p = 0.6794; Treatment $F_{(1,8)}$ = 44.75, p = 0.0002; Genotype $F_{(1,8)}$ = 29.50, p = 0.0006) with Tukey's post-hoc test for n = 3 independent experiments. * p < 0.05, ** p < 0.01. Scale bar: 50 μm. βIII tubulin: red, GFP: green, Hoechst: blue.

(Met: Metformin, Scr-sh: Scramble shRNA, Mgll-sh: Mgll shRNA; CM-WT/Scr-sh: CM from WT NPCs transfected with Scr-sh; CM-WT/Mgll-sh: CM from WT NPCs transfected with Mgll-sh; CM-CBPS436A/Scr-sh: CM from CBPS436A NPCs transfected with Scr-sh; CM-CBPS436A/Mgll-sh: CM from CBPS436A NPCs transfected with Mgll-sh). All NPC differentiation assays were performed in the presence of 1 μM metformin.

4.3. Mgll inhibition rescues hippocampal neurogenesis deficits in CBPS436A mice *in vivo*

Our recent study showed that the aPKC-CBP pathway is fully active in the murine hippocampus at the age of 6 months, and that phospho-null CBPS436A mice exhibit significant hippocampal neuronal differentiation defects at the age of 6 months (Gouveia *et al.*, 2016).

To determine if the hippocampal neurogenesis deficits in 6-month-old CBPS436A mice are the result of elevated Mgll levels (**Figure 1 C**), I treated 6-month-old CBPS436A mice with a selective inhibitor of Mgll activity, JZL-184, for two weeks and assessed its effect on hippocampal neuronal differentiation. These mice were also given BrdU injections at days 3-5 to label dividing cells. Following 14 days of drug treatment, the mice were sacrificed, and their hippocampal brain sections were immunostained for BrdU and NeuN (a mature neuronal marker) (**Figure 6 A**). The percentage of $NeuN^+/BrdU^+$ neurons out of total $BrdU^+$ cells was quantified. Consistent with previous findings (Gouveia *et al.*, 2016), I observed a significant neuronal differentiation deficit in 6-month-old CBPS436A mice as compared to their WT littermates in the vehicle (control) group, measured by a decreased population of $NeuN^+/BrdU^+$ newborn neurons (**Figure 6**). Importantly, the CBPS436A mice that received JZL-184 treatment displayed a restored population of newborn neurons ($NeuN^+/BrdU^+$) back to basal levels observed in WT mice (**Figure 6 B**). This illustrates that inhibition of Mgll activity by JZL-184 is able to rescue the hippocampal neuronal differentiation deficits in the 6-month-old CBPS436A mice.

A

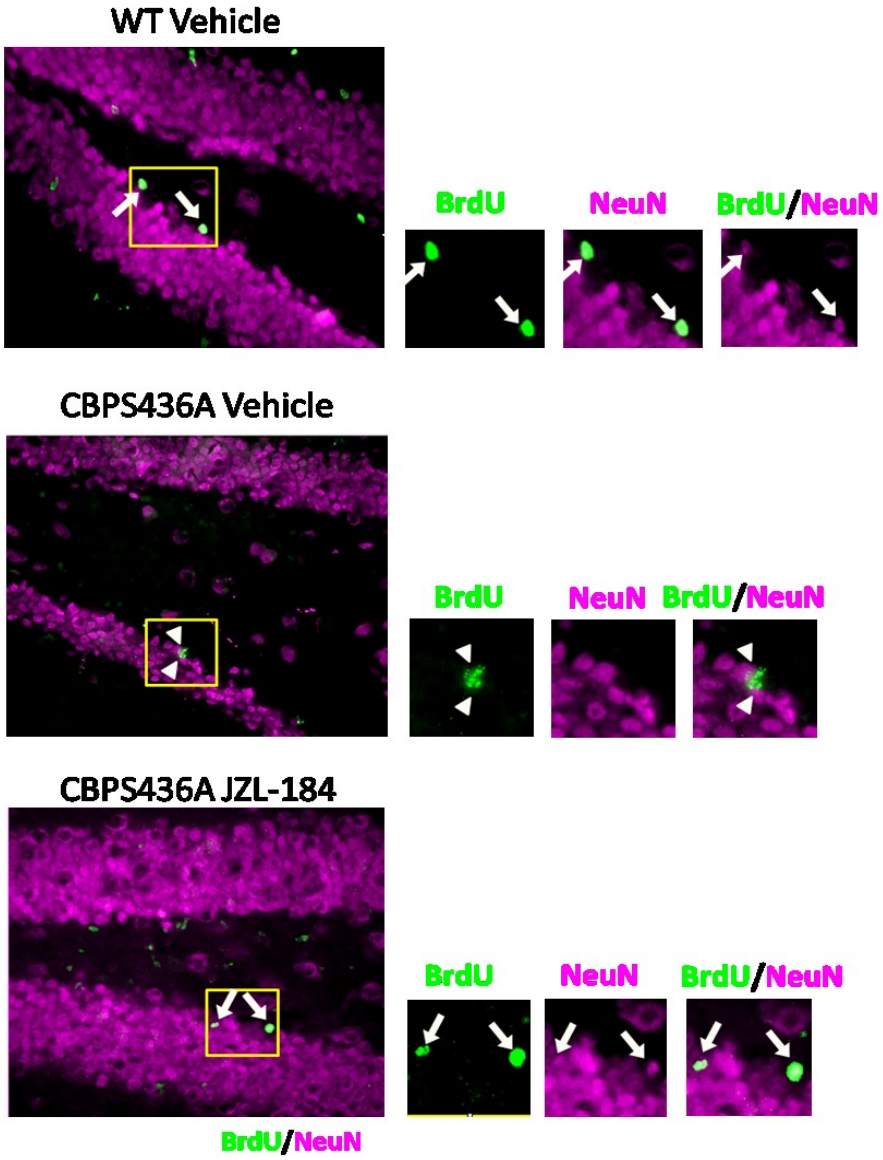
WT Vehicle
BrdU
NeuN
BrdU/NeuN
CBPS436A Vehicle
BrdU
NeuN
BrdU/NeuN
CBPS436A JZL-184
BrdU
NeuN
BrdU/NeuN
BrdU/NeuN

B

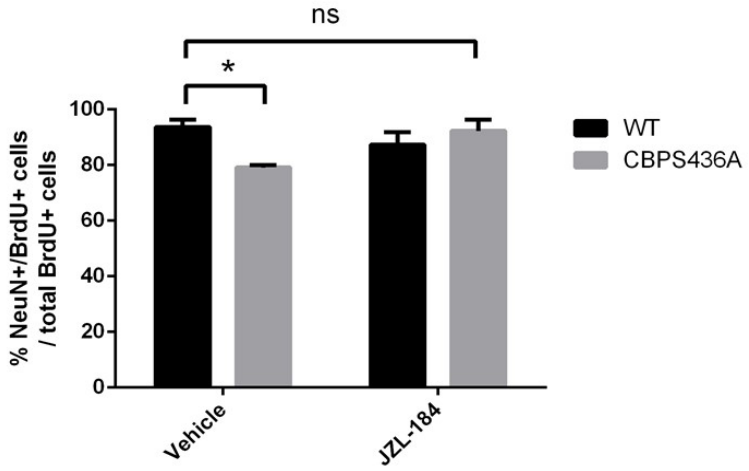
ns
*
% NeuN+/BrdU+ cells / total BrdU+ cells
100
80
60
40
20
0
Vehicle
JZL-184
WT
CBPS436A

Figure 6: Inhibition of Mgll activity with JZL-184 rescues hippocampal neurogenesis deficits in CBPS436A mice. (A) Immunofluorescent images of hippocampal sections from 6-month-old WT and CBPS436A mice injected with JZL-184 (or vehicle) and BrdU, immunostained for BrdU (green) and NeuN (purple). Arrows denote $NeuN^+/BrdU^+$ co-labelled cells; arrowheads denote $BrdU^+$ cells. **(B)** Quantitative analysis of the percentage of newborn neurons ($NeuN^+/BrdU^+$) out of total $BrdU^+$ cells in the hippocampal dentate gyrus following BrdU pulse-labelling from both WT and CBPS436A mice treated with vehicle and JZL-184. Statistical analysis was performed for n = 3 samples per group using two-way ANOVA (Genotype x treatment $F_{(1,8)} = 8.615$, $p = 0.0188$; Genotype $F_{(1,8)} = 2.082$, $p = 0.1870$; Treatment $F_{(1,8)} = 1.043$, $p = 0.3369$) with Tukey's post-hoc test. * $p < 0.05$.

4.4. Late passage NPCs display intrinsic activation of the aPKC-CBP pathway

Previous work shows that metformin activates the aPKC-CBP pathway to promote adult NPC differentiation *in vitro* (Fatt *et al.*, 2015). We have now identified that continued passaging of NPCs is another approach to activate the aPKC-CBP pathway in culture.

I continued to passage WT and CBPS436A NPCs until passage 5 (P5) and compared the status of the aPKC-CBP pathway in these late passage P5 NPCs relative to their early passage P2 counterparts. I observed that there was a marked variation in total aPKC (T-aPKC) levels in both WT and CBPS436A P5 NPCs relative to their respective P2 NPCs, although no change was apparent overall (**Figure 7 A, B**). Given this variability, I assessed aPKC activity using an active form of aPKC, phosphorylated-T410/403 aPKC (pT410/403-aPKC; p-aPKC), normalized to GAPDH. I showed that both WT and CBPS436A P5 NPCs exhibited elevated aPKC activity compared to their respective P2 counterparts (**Figure 7 A, C**), suggesting an intrinsic activation of the aPKC-CBP pathway in the P5 NPCs.

Interestingly, both WT and CBPS436A P5 NPCs exhibited higher Mgll levels than their P2 counterparts, despite enhanced aPKC activity (**Figure 7 D**). Importantly, Mgll levels in the CBPS436A P5 NPCs were significantly higher than those in the WT P5 NPCs (**Figure 7 D**), reminiscent of Mgll expression in differentiating CBPS436A and WT P2 NPCs in the presence of metformin (**Figure 2**).

These findings suggest that continued passaging of NPCs is able to intrinsically activate the aPKC-CBP pathway to repress Mgll expression, thus, representing an additional culture model to study the role of this pathway in regulating NPC function.

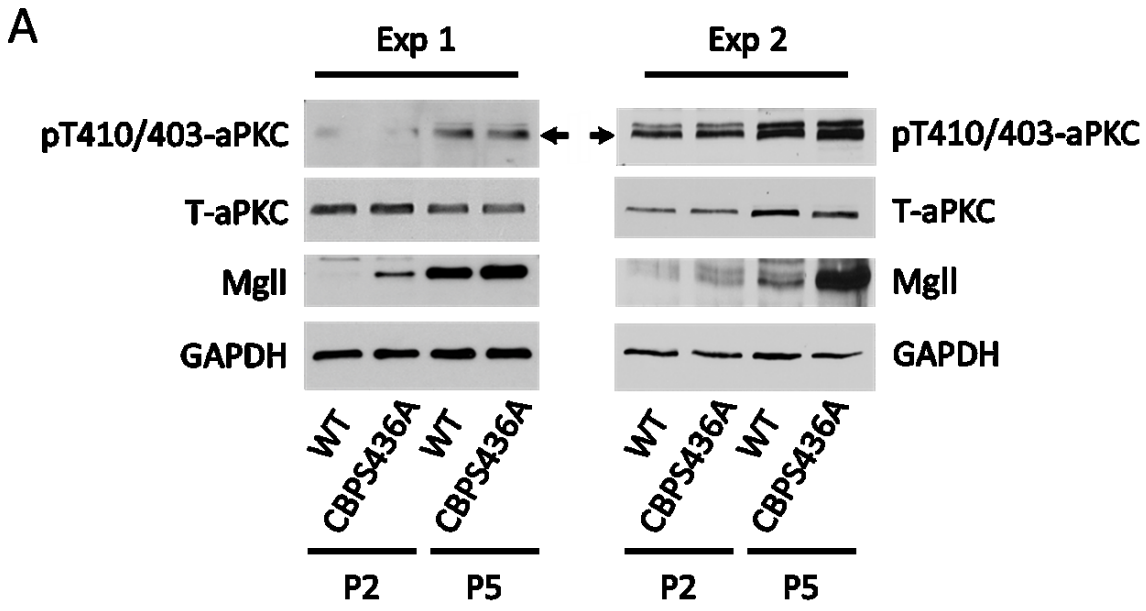
A
Exp 1
Exp 2
pT410/403-aPKC
T-aPKC
MgII
GAPDH
pT410/403-aPKC
T-aPKC
MgII
GAPDH
WT
CBPS436A
WT
CBPS436A
WT
CBPS436A
WT
CBPS436A
P2
P5
P2
P5

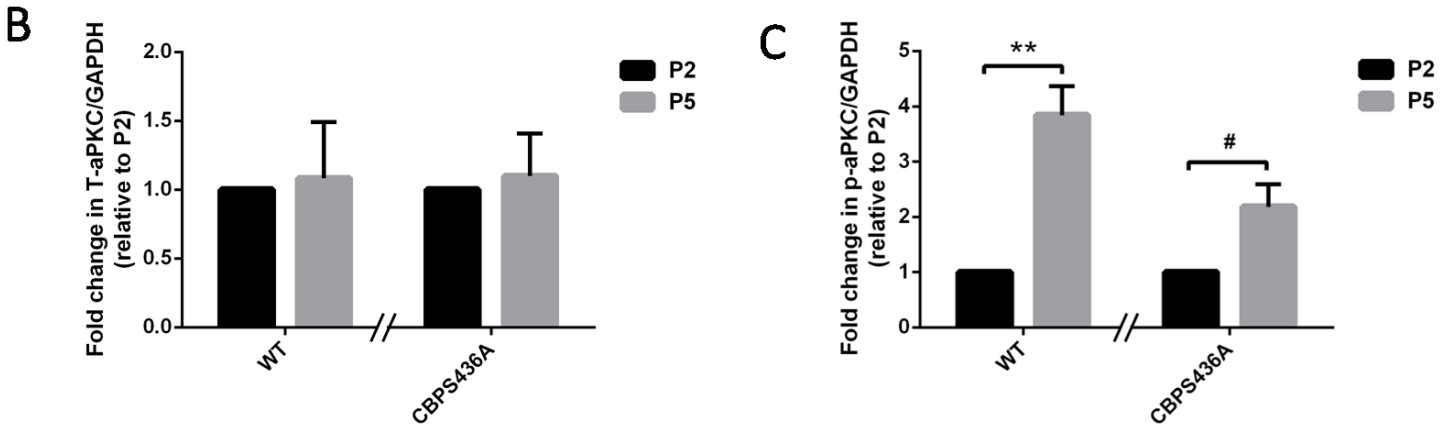
B
Fold change in T-aPKC/GAPDH (relative to P2)
2.0
1.5
1.0
0.5
0.0
P2
P5
WT
CBPS436A
C
Fold change in p-aPKC/GAPDH (relative to P2)
5
4
3
2
1
0
**
#
P2
P5
WT
CBPS436A

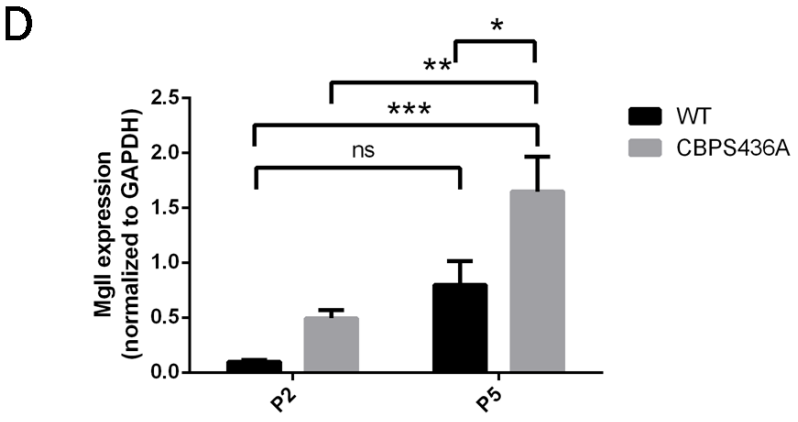
D
MgII expression (normalized to GAPDH)
2.5
2.0
1.5
1.0
0.5
0.0
*
**
***
ns
WT
CBPS436A
P2
P5

Figure 7: Late passage CBPS436A NPCs display intrinsic activation of aPKC-CBP pathway. (A) Representative western blot images of total protein lysates from proliferating P2 (early passage) and P5 (late passage) WT and CBPS436A NPCs, probed for Mgll and pT410/403-aPKC (p-aPKC), and re-probed for T-aPKC and GAPDH (a loading control) from two independent experiments. **(B)** Quantitative analysis of T-aPKC expression relative to GAPDH in proliferating WT and CBPS436A P2 and P5 NPCs. Data analyzed by Student's t-test for n = 4 independent experiments. **(C)** Quantitative analysis of aPKC activity measured as p-aPKC (pT410/403-aPKC) protein expression relative to GAPDH in proliferating WT and CBPS436A P2 and P5 NPCs. Data analyzed by Student's t-test for n = 4 independent experiments. **(D)** Quantitative analysis of Mgll expression relative to GAPDH in WT and CBPS436A P2 and P5 NPCs. Data was analyzed by two-way ANOVA (Genotype x passage $F_{(1,12)} = 1.315$, $p = 0.2739$; Genotype $F_{(1,12)} = 22.03$, $p = 0.0005$; Passage $F_{(1,12)} = 9.920$, $p = 0.0084$) with Tukey's post-hoc test for 4 independent experiments. * $p < 0.05$, ** $p < 0.01$, *** $p < 0.001$, $^{\#}$ $p < 0.06$, ns = not significant.

4.5. 3xTg NPCs exhibit an impaired aPKC-CBP mediated Mgll repression

Previous studies have reported decreased PKC activation in post-mortem AD brains (Crary *et al.*, 2006; Etcheberrigaray *et al.*, 2004). Interestingly, Mgll was recently identified as a therapeutic target for AD (Chen *et al.*, 2012). These findings along with our initial results, prompted us to ask if aPKC-CBP mediated Mgll repression was impaired in AD NPCs. For this, I assessed the status of the aPKC-CBP pathway in proliferating P2 NPCs derived from 3xTg mice. I observed a significant decrease in both T-aPKC and pT410/403-aPKC levels in the 3xTg NPCs as compared to the Non-Tg NPCs (**Figure 8**). Further, 3xTg NPCs also exhibited elevated Mgll levels as compared to the Non-Tg NPCs (**Figure 8**). These findings were consistent with previous reports that have shown impaired aPKC and Mgll upregulation in AD and thus, indicate that SVZ neurosphere cultures are a suitable model to study the impaired pathway in context of AD.

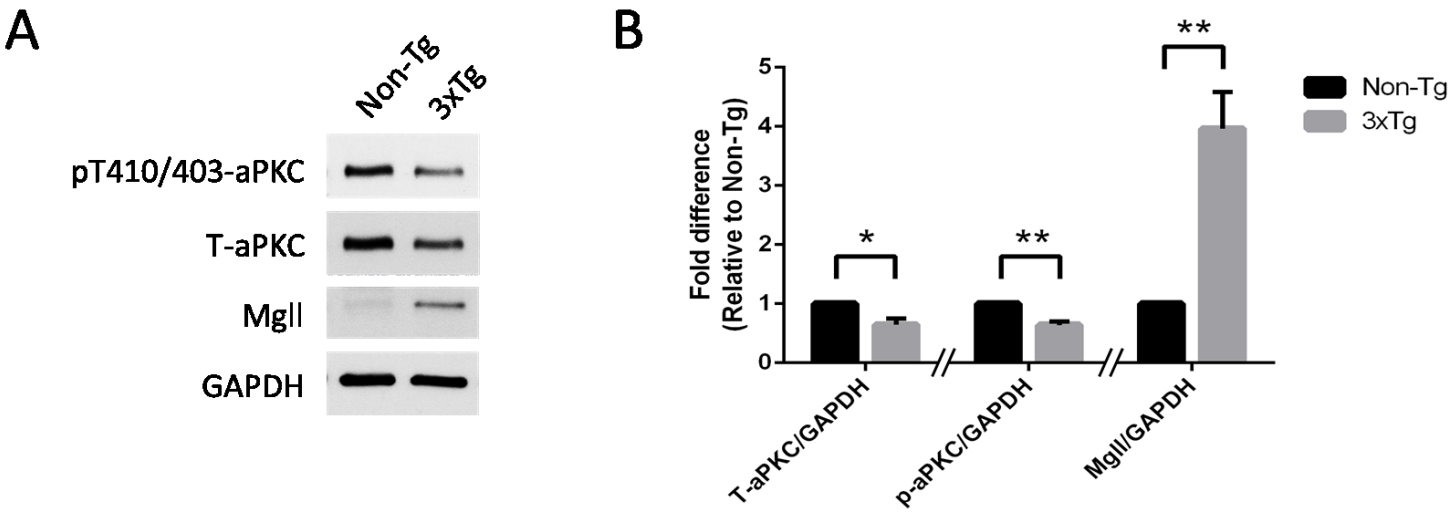

Figure 8: 3xTg NPCs display reduced aPKC levels and elevated Mgll levels. (A) Representative western blot images of total protein lysates from proliferating Non-Tg and 3xTg P2 NPCs, probed for Mgll, pT410/403-aPKC (p-aPKC), and re-probed for T-aPKC and GAPDH (a loading control). **(B)** Quantitative analysis of T-aPKC, p-aPKC and Mgll protein levels relative to GAPDH in 3xTg NPCs as compared to Non-Tg NPCs. Data was quantified from 5 independent experiments using paired Student's t-test. * $p < 0.05$, ** $p < 0.01$.

4.6. The attenuation of aPKC-CBP mediated Mgll repression leads to increased NPC proliferation at the expense of their neuronal differentiation

Since Mgll activity hydrolyses 2-AG to produce ARA, two known bioactive lipids that promote NPC neuronal differentiation and proliferation, respectively, (Prenderville *et al.* 2015, Maekawa *et al.*, 2009; Sakayouri *et al.*, 2011; Jin *et al.*, 2004b), I examined proliferation versus differentiation of the CBPS436A and 3xTg NPCs as an outcome of increased Mgll expression observed in these NPCs.

I used the CBPS436A P5 NPCs and 3xTg P2 NPCs, both of which display elevated Mgll levels (**Figure 7 D; Figure 8 B**) to examine NPC proliferation and differentiation. Proliferation was assessed by measuring the distribution of neurospheres on the basis of size, while neuronal differentiation was assessed by quantifying the percentage of βIII tubulin$^+$ newborn neurons produced from the same group of NPCs when treated with differentiation conditions.

In both CBPS436A P5 and 3xTg P2 NPC-derived neurospheres there was a shift towards a higher percentage of large neurospheres (>150 µm) compared to WT P5 and Non-Tg P2 NPC-derived neurospheres, respectively. Correspondingly, a significant decrease in the percentage of small neurospheres (<50 µm) in CBPS436A P5 NPCs and a decrease in the percentage of mid-sized (50-150 µm) neurospheres in the 3xTg P2 NPCs was observed (**Figure 9 A, B; Figure 10 A**, **B**) Interestingly, this increased proliferation in both CBPS436A P5 and 3xTg P2 NPCs was concurrently associated with reduced neuronal differentiation (**Figure 9 C, D; Figure 10 C, D**), measured by a decreased percentage of βIII tubulin$^+$ neurons produced from CBPS436A P5 and 3xTg P2 NPCs.

To ask whether increased ARA-GPR40 signaling, a pathway known to promote primate NPC proliferation (Boneva and Yamashima, 2012), is responsible for the enhanced proliferation observed in the CBPS436A P5 and 3xTg P2 NPCs, I treated these NPCs with a potent GPR40 antagonist, DC260126. The results showed that 100 nM DC260126 was able to reverse the increased neurosphere size from CBPS436A P5 and 3xTg P2 NPCs back to basal levels but did not have significant effects on WT and Non-Tg NPCs (**Figure 9 B; Figure 10 B**). These results support that elevated Mgll levels in the CBPS436A P5 and 3xTg P2 NPCs promote NPC proliferation by activating ARA-GPR40 signaling.

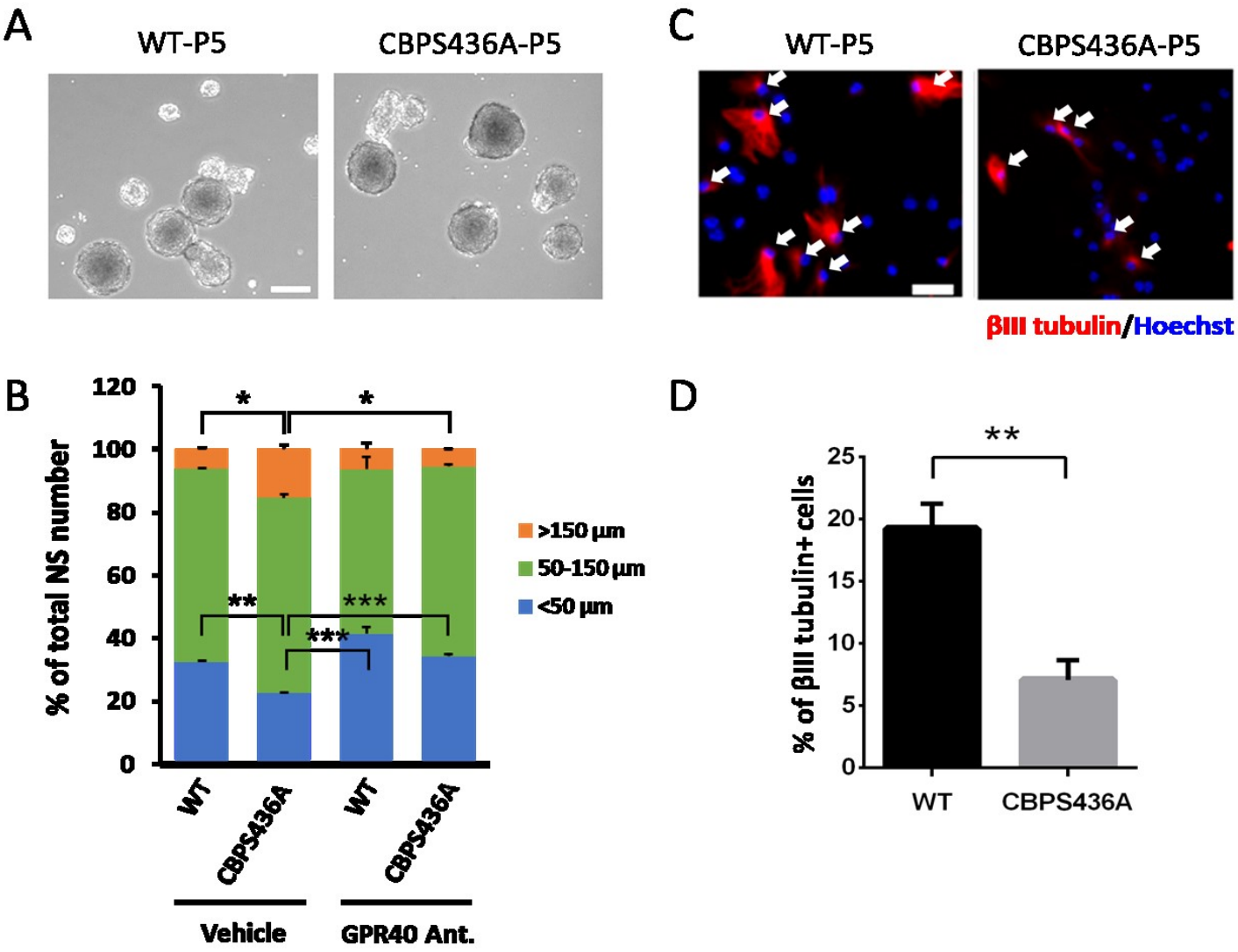

Figure 9: Late passage CBPS436A P5 NPCs exhibit enhanced proliferation, concurrently with reduced differentiation. (A) Representative bright-field images of WT and CBPS436A P5 neurospheres. Scale bar: 200 µM. **(B)** Quantitative analysis of the percentage of small (<50 µm), mid-sized (50-150 µm), and large (>150 µm) neurospheres generated from WT and CBPS436A P5 NPCs, treated with vehicle (0.01% DMSO) and GPR40 antagonist (100 nM DC260126). Statistical analysis was performed for n=3 independent experiments using two-way ANOVA with Tukey's post-hoc test for each size bracket (<50 µm: Genotype x treatment $F_{(1,8)}$ = 1.161, p = 0.3126; Genotype $F_{(1,8)}$ = 46.58, p = 0.0001; Treatment $F_{(1,8)}$ = 66.82, p < 0.0001)(50-150 µM: Genotype x treatment $F_{(1,8)}$ = 3.274, p = 0.1080; Genotype $F_{(1,8)}$ = 4.718, p = 0.0616; Treatment $F_{(1,8)}$ = 6.596, p = 0.0332)(>150 µM: Genotype x treatment $F_{(1,8)}$ = 6.238, p = 0.0371; Genotype $F_{(1,8)}$ = 4.135, p = 0.0764; Treatment $F_{(1,8)}$ = 6.094, p = 0.0388). **(C)** Representative immunofluorescent images of

differentiating WT and CBPS436A P5 NPCs, immunostained for βIII tubulin (red) and Hoechst (blue). Scale bar: 80 µM. **(D)** Quantitative analysis of the percentage of βIII tubulin^{+} neurons generated from WT and CBPS436A P5 NPCs at 7 DIV upon differentiation. Data was quantified for 3 independent experiments using Student's t-test. * indicates $p < 0.05$; ** indicates $p < 0.01$.

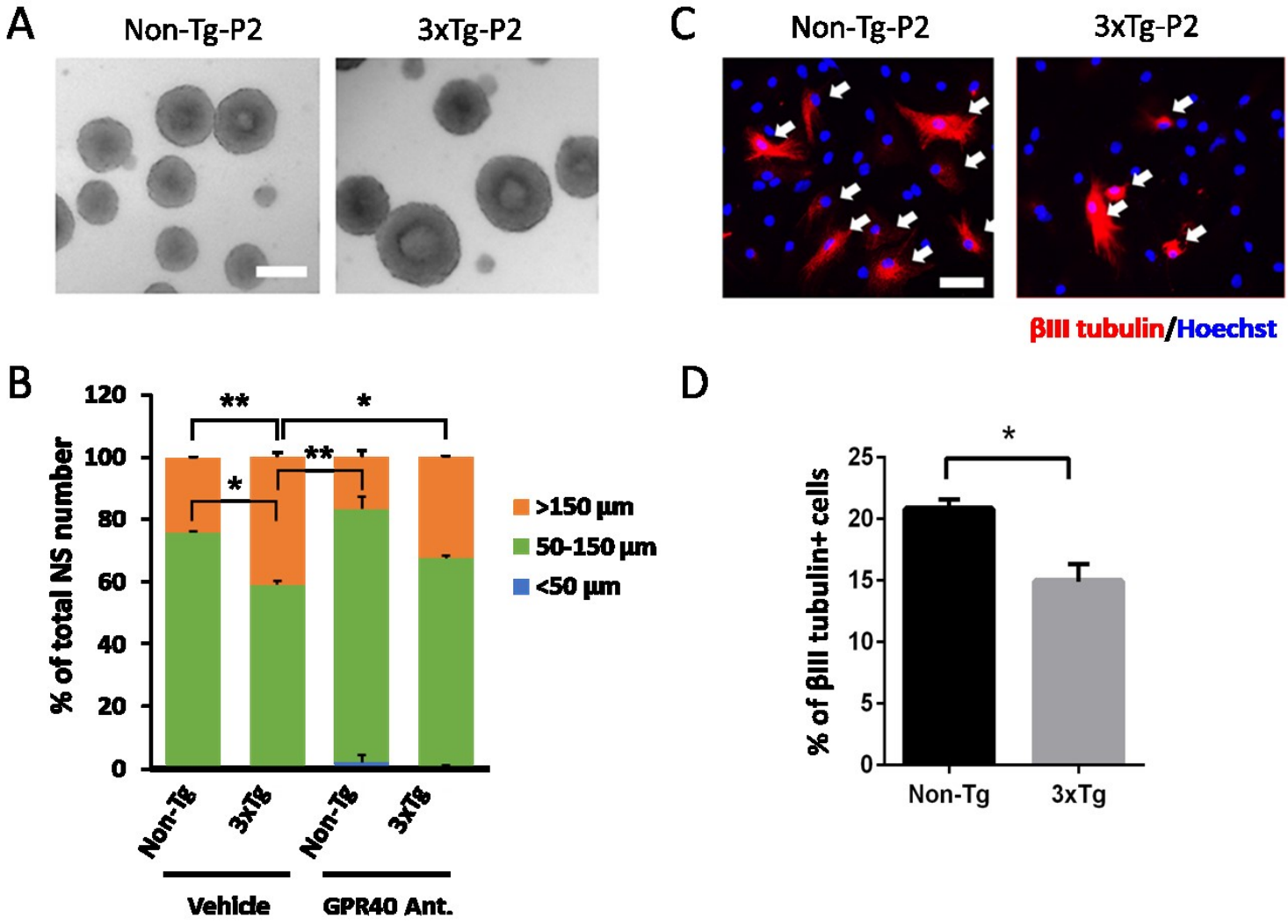

Figure 10: Early passage 3xTg P2 NPCs exhibit enhanced proliferation, concurrently with reduced differentiation. (A) Representative bright-field images of Non-Tg and 3xTg P2 neurospheres. Scale bar: 200 µM. **(B)** Quantitative analysis of the percentage of small (<50 µm), mid-sized (50-150 µm), and large (>150 µm) neurospheres generated from Non-Tg and 3xTg P2 NPCs, treated with vehicle (0.01% DMSO) and GPR40 antagonist (100 nM DC260126). Statistical analysis was performed for n=3 independent experiments using two-way ANOVA with Tukey's post-hoc test for each size bracket (<50 µm: Genotype x treatment $F_{(1,8)}$ = 0.3945, p = 0.5640; Genotype $F_{(1,8)}$ = 0.5295, p = 0.5071; Treatment $F_{(1,8)}$ = 1.127, p = 0.3482)(50-150 µM: Genotype x treatment $F_{(1,8)}$ = 0.3917, p = 0.5653; Genotype $F_{(1,8)}$ = 51.96, p = 0.002; Treatment $F_{(1,8)}$ = 9.647, p = 0.036)(>150 µM: Genotype x treatment $F_{(1,8)}$ = 0.3010, p = 0.6124; Genotype $F_{(1,8)}$ = 198.4, p = 0.0001; Treatment $F_{(1,8)}$ = 46.24, p = 0.0024). **(C)** Representative immunofluorescent images of

differentiating Non-Tg and 3xTg P2 NPCs stained for βIII tubulin (red) and Hoechst (blue). Scale bar: 80 µM. **(D)** Quantitative analysis of the percentage of βIII tubulin^{+} neurons generated from Non-Tg and 3xTg P2 NPCs at 7 DIV upon differentiation. Data was quantified for 3 independent experiments using Student's t-test. * $p < 0.05$, ** $p < 0.01$.

4.7. Mgll knockdown rescues neuronal differentiation deficits in late passage CBPS436A NPCs

Since the CBPS436A P5 NPCs display a reduced neuronal differentiation (**Figure 9 D**) concurrently with increased Mgll expression (**Figure 7 D**), I asked whether Mgll knockdown could rescue this differentiation deficit. To test this, I transfected WT and CBPS436A P5 NPCs with Mgll or Scr shRNAs, together with an eGFP plasmid. As expected, I observed a significant differentiation deficit in the CBPS436A P5 NPCs relative to the WT P5 NPCs in the Scr shRNA (control) condition, which was rescued upon genetic knockdown of Mgll (**Figure 11**). These results confirm that elevated Mgll expression in the CBPS436A P5 NPCs is responsible for their neuronal differentiation impairments.

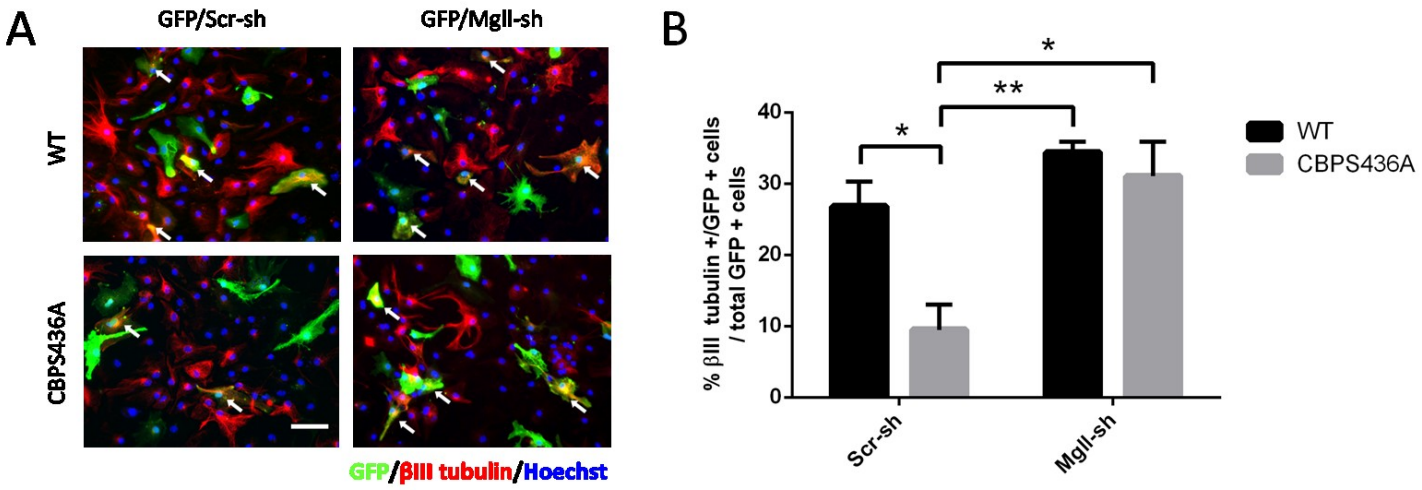

Figure 11: Mgll knockdown rescues neuronal differentiation deficits in late passage P5 CBPS436A NPCs. (A) Representative immunofluorescent images of differentiating WT and CBPS436A P5 NPCs, following transfection with Mgll or Scr shRNAs together with an eGFP plasmid, immunostained for GFP (green), βIII tubulin (red) and Hoechst (blue). **(B)** Quantification of the percentage of βIII tubulin^{+}/GFP^{+} co-labelled neurons generated from transfected NPCs. Statistical analysis was performed for n = 3 independent experiments using Two-way ANOVA (Genotype x treatment $F_{(1,8)}$ = 4.952, p = 0.0520; Genotype $F_{(1,8)}$ = 8.556, p = 0.0191; Treatment $F_{(1,8)}$ = 17.03, p = 0.0033) with Tukey's post-hoc test. * p < 0.05, ** p < 0.01. Scale bar: 75 µm. (Scr-sh: Scramble shRNA, Mgll-sh: Mgll shRNA).

4.8. Reactivation of the aPKC-CBP mediated Mgll repression rescues differentiation deficits in 3xTg NPCs

To assess if the impaired aPKC-CBP mediated Mgll repression is responsible for neuronal differentiation deficits observed in the 3xTg NPCs (**Figure 9 C, D**), I examined whether reactivation of the pathway at different molecular levels would recover the differentiation defects of these NPCs.

First, I treated the Non-Tg and 3xTg P2 NPCs with metformin (500 nM) to directly activate the aPKC-CBP pathway and assessed the changes in neuronal differentiation by immunostaining for βIII tubulin. The results revealed that metformin treatment rescued the 3xTg NPC neuronal differentiation deficit, shown by a significant increase in the percentage of βIII tubulin$^+$ neurons generated from 3xTg NPCs back to the basal levels observed in the Non-Tg NPCs (**Figure 12 A, B**).

Next, I transfected Non-Tg and 3xTg P2 NPCs with the phosphomimic CBPS436D plasmid to achieve a constitutive activation of aPKC-CBP pathway before directing these NPCs towards differentiation. Immunostaining for βIII tubulin at 7 DIV showed a consistent neuronal differentiation deficit in the 3xTg NPCs as compared to the Non-Tg NPCs, transfected with the empty vector pcDNA3.1 (**Figure 12 C, D**) as expected. Interestingly, I observed a significant increase in the generation of βIII tubulin$^+$ newborn neurons from 3xTg NPCs transfected with the phosphomimic CBPS436D plasmid (**Figure 12 C, D**). In addition, I transfected Non-Tg and 3xTg P2 NPCs with Mgll shRNAs or Scr shRNA (as a transfection control) to knockdown Mgll levels. As

expected, I observed the same rescue effect on 3xTg NPC neuronal differentiation deficits upon Mgll knockdown as overexpression of CBPS346D plasmid (**Figure 12 E**).

Finally, I treated Non-Tg and 3xTg P2 NPCs with JZL-184 (1 μM), a selective inhibitor of Mgll activity. I observed that JZL-184 treatment also significantly increased the percentage of βIII tubulin$^+$ neurons generated from 3xTg NPCs relative to the vehicle (0.1% DMSO), and back to the basal levels observed in the Non-Tg NPCs (**Figure 12 F**).

These data thus show that both reactivation of the aPKC-CBP pathway and removal of Mgll level/activity can alleviate the neuronal differentiation deficits in 3xTg NPCs.

To further assess the role of 2-AG-eCBR signaling in regulating NPC differentiation in 3xTg NPCs, I treated Non-Tg and 3xTg P2 NPCs with eCBR1 and eCBR2 agonists, ACEA (1 μM) and JWH133 (1 μM), respectively. Consistent with the previous results, I observed a significant reduction in the percentage of βIII tubulin$^+$ neurons generated from 3xTg NPCs as compared to Non-Tg NPCs in the vehicle (0.1% DMSO) group (**Figure 13**). This differentiation defect in 3xTg NPCs was rescued upon treatment with eCBR2 agonist (JHWH133) but not with eCBR1 agonist (ACEA) (**Figure 13**).

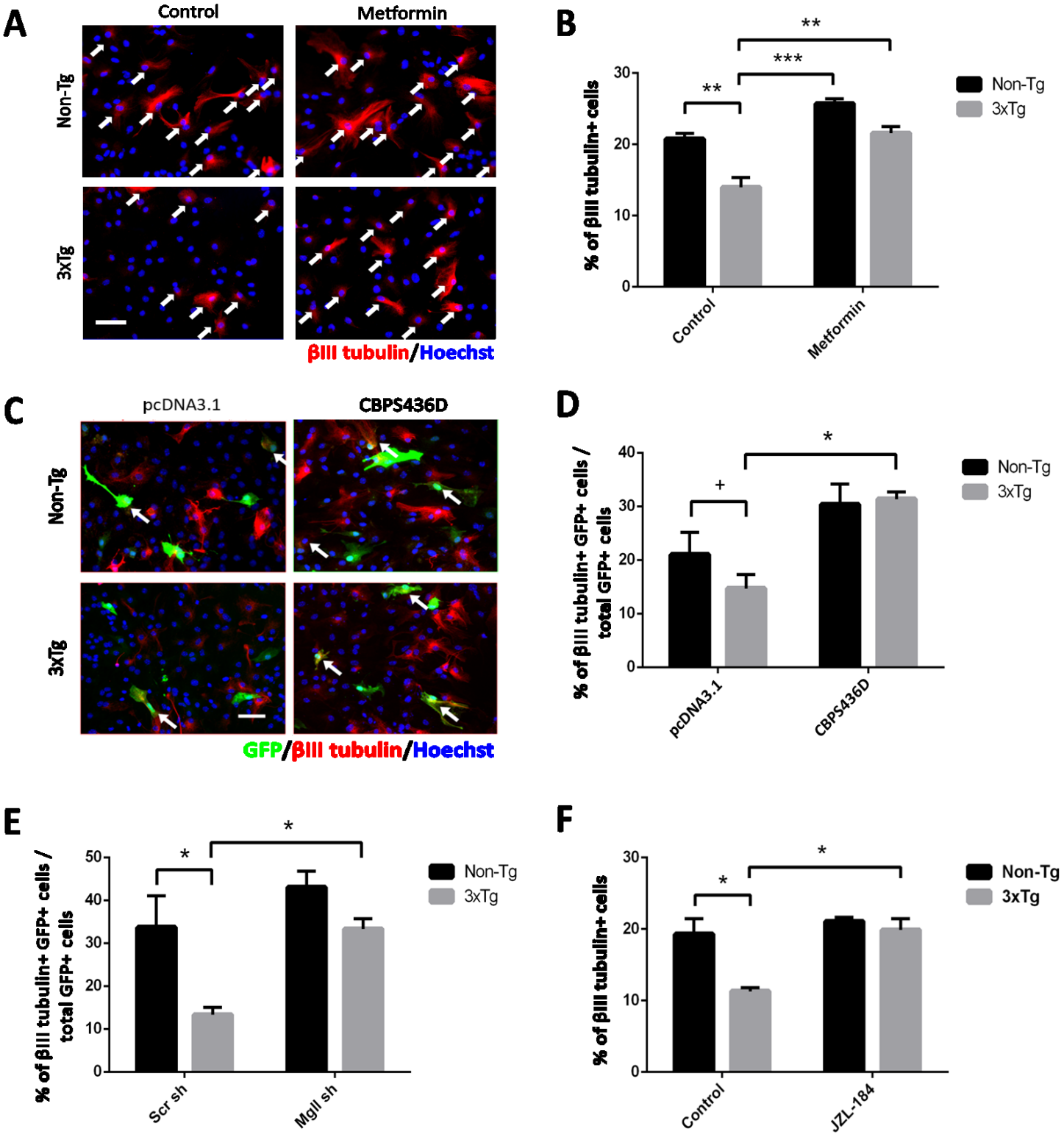
A
Control
Metformin
Non-Tg
3xTg
βIII tubulin/Hoechst
B
% of βIII tubulin+ cells
Non-Tg
3xTg
Control
Metformin
C
pcDNA3.1
CBPS436D
Non-Tg
3xTg
GFP/βIII tubulin/Hoechst
D
% of βIII tubulin+ GFP+ cells / total GFP+ cells
Non-Tg
3xTg
pcDNA3.1
CBPS436D
E
% of βIII tubulin+ GFP+ cells / total GFP+ cells
Non-Tg
3xTg
Scr sh
MgII sh
F
% of βIII tubulin+ cells
Non-Tg
3xTg
Control
JZL-184

Figure 12: Reactivation of aPKC-CBP mediated Mgll repression rescues neuronal differentiation defects in 3xTg NPCs. (A) Representative immunofluorescent images of differentiating Non-Tg and 3xTg P2 NPCs, treated with control (water) or metformin and immunostained for βIII tubulin (red) and Hoechst (blue). **(B)** Quantification of the percentage of βIII tubulin^{+} neurons generated from Non-Tg and 3xTg P2 NPCs at 7 DIV differentiation in the absence and presence of metformin (500 nM). Data analyzed by two-way ANOVA (Genotype x treatment $F_{(1,8)}$ = 1.532, p = 0.244; Genotype $F_{(1,8)}$ = 34.29, p = 0.0002; Treatment $F_{(1,8)}$ = 25.97, p = 0.0005, n = 3) with Tukey's post-hoc test. **(C)** Representative immunofluorescent images of differentiating Non-Tg and 3xTg NPCs, transfected with CBPS436D or empty vector pcDNA3.1 together with an eGFP plasmid, and immunostained for GFP (green), βIII tubulin (red) and Hoechst (blue). **(D)** Quantification of the percentage of βIII tubulin^{+}/GFP^{+} co-labelled neurons generated from total transfected NPCs, following transfection with CBPS436D or pcDNA3.1 plasmids. Data analyzed by two-way ANOVA (Genotype x treatment $F_{(1,8)}$ = 1.674, p = 0.2318; Genotype $F_{(1,8)}$ = 0.9419, p = 0.3602; Treatment $F_{(1,8)}$ = 18.60, p = 0.0026, n = 3) with Tukey's post-hoc test. **(E)** Quantification of the percentage of βIII tubulin^{+}/GFP^{+} co-labelled neurons generated from total transfected NPCs following transfection with Mgll or Scr shRNAs. Data analyzed by two-way ANOVA (Genotype x treatment $F_{(1,8)}$ = 1.791, p = 0.2176; Genotype $F_{(1,8)}$ = 12.64, p = 0.0074; Treatment $F_{(1,8)}$ = 12.11, p = 0.0083, n = 3) with Tukey's post-hoc test. **(F)** Quantification of the percentage of βIII tubulin^{+} neurons generated from Non-Tg and 3xTg P2 NPCs at 7 DIV upon differentiation in the presence of vehicle (0.1% DMSO) or JZL-184 (1 µM). Data analyzed by two-way ANOVA (Genotype x treatment $F_{(1,8)}$ = 5.896, p = 0.0721; Genotype $F_{(1,8)}$ = 10.88, p = 0.03; Treatment $F_{(1,8)}$ = 13.69, p = 0.0208, n = 3) with Tukey's post-hoc test. $^{+}$ p = 0.05, * p < 0.05, ** p < 0.01, *** p < 0.001. Scale bar: 50 µM.

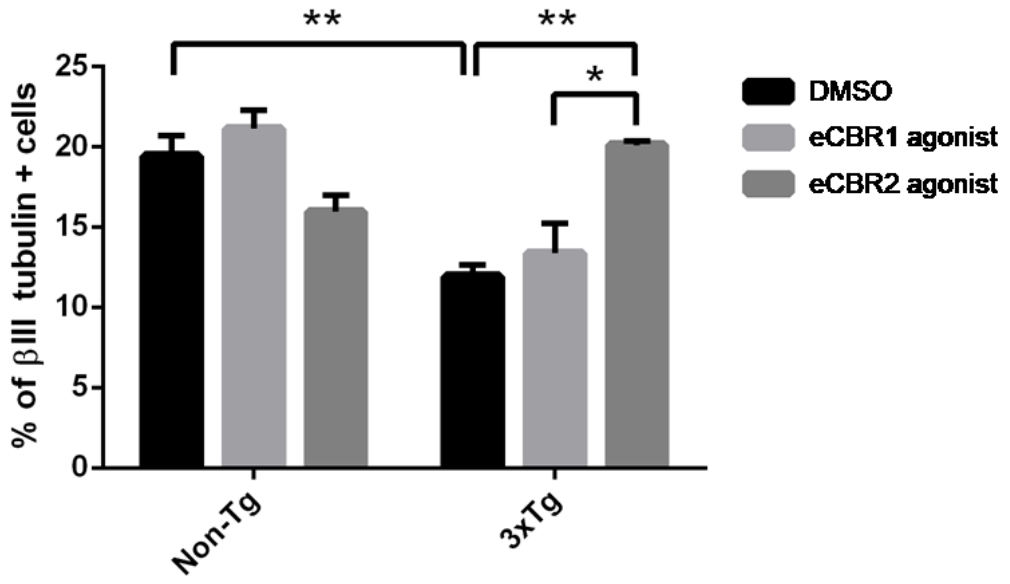

Figure 13: The endocannabinoid pathway mediates neuronal differentiation in 3xTg NPCs. Quantitative analysis of the percentage of βIII tubulin^{+} neurons generated from Non-Tg and 3xTg P2 NPCs treated with eCBR1 and eCBR2 agonists, ACEA (1 µM) and JWH133 (1 µM), and vehicle (0.1% DMSO). Statistical analysis was performed using two-way ANOVA (Genotype x treatment $F_{(2,12)} = 14.77$, $p = 0.0008$; Genotype $F_{(1,12)} = 14.12$, $p = 0.0032$; Treatment $F_{(2,12)} = 1.950$, $p = 0.1884$) with Tukey's post-hoc test for n = 3 independent experiments. * $p < 0.05$, ** $p < 0.01$.

5. Discussion

This study defines a role for epigenetic regulation of lipid metabolism in determining adult NPC fate. Specifically, I show that activation of the aPKC-CBP pathway by metformin or continued passaging represses the expression of Mgll, a lipase that breaks down 2-AG to produce ARA, in adult NPCs. Attenuation of the aPKC-CBP pathway in phospho-null CBPS436A mice and the 3xTg AD mouse model results in elevated Mgll expression in their SVZ NPCs, which in turn exhibit increased NPC proliferation at the expense of neuronal differentiation. I further delineate that activation of ARA-GPR40 signaling is responsible for increased proliferation in both the CBPS436A and 3xTg NPCs, while reduced 2-AG-eCBR signaling is responsible for decreased neuronal differentiation in the 3xTg NPCs. Lastly, I show that knockdown of Mgll and/or inhibition of its activity is able to rescue neuronal differentiation deficits of CBPS436A NPCs both *in vitro* and *in vivo*, and that reactivation of the aPKC-CBP mediated Mgll repression is capable of restoring neuronal differentiation in 3xTg mice. These findings support that the aPKC-CBP mediated Mgll repression is essential for normal NPC function, and that when perturbed in AD, it causes impaired neurogenesis, contributing to AD predisposition.

5.1. The aPKC-CBP pathway directly regulates Mgll expression

Mgll is an important lipase that breaks down the endocannabinoid 2-AG to produce ARA, a major precursor for the inflammatory eicosanoids (Blankman *et al.*, 2007; Khanpure *et al.*, 2007; Normura *et al.*, 2011). Thus, by hydrolyzing 2-AG, Mgll not only alters 2-AG signaling but also modulates the ARA-mediated inflammatory processes in the brain. Given its involvement in the

regulation of these critical lipid signaling pathways with diverse physiological functions, Mgll has been considered an important target for neuroinflammatory and neurodegenerative disorders (Fowler *et al.*, 2012; Mulvihill and Normura, 2014; Grabner *et al.*, 2016). Despite this importance of Mgll in both physiological and pathological conditions, it is still not known how Mgll is regulated. In this regard, my study elucidates a novel epigenetic mechanism that regulates Mgll expression at a transcriptional level. Unpublished work from other lab members shows that activation of the aPKC-CBP pathway directly represses Mgll expression by reducing CBP binding at the Mgll promoter (**Figure 1**). I further demonstrate that attenuation of the aPKC-CBP pathway is associated with elevated Mgll levels and increased histone acetylation at a site catalyzed by CBP (H2BK5) (Valor *et al.*, 2011) (**Figure 2; Figure 3**). These findings provide an insight into the epigenetic regulation of Mgll expression, and thus pave the way for developing potential therapeutic approaches that repress Mgll expression by targeting the aPKC-CBP pathway.

5.2. Mgll acts in cell intrinsic and cell extrinsic manners

Our lab previously showed that phospho-null CBPS436A NPCs do not respond to metformin to promote neuronal differentiation of adult SVZ NPCs (Fatt *et al.*, 2015). Intriguingly, my results show that Mgll knockdown rescues the neuronal differentiation deficits of CBPS436A NPCs in response to metformin and that these effects are mediated in both cell-intrinsic and cell-extrinsic manners (**Figure 5**). These rescue effects on neuronal differentiation upon Mgll knockdown, are likely an outcome of enhanced 2-AG-eCBR signaling, which has been extensively

shown to promote NPC differentiation (Jin *et al.*, 2004b; Díaz-Alonso *et al.*, 2012; Xapelli *et al.*, 2013; Compagnucci *et al.*, 2013).

2-AG is a hydrophobic lipid, that can freely diffuse across the cell membrane, however, how it traverses the extracellular hydrophilic environment to promote NPC differentiation in a cell-extrinsic manner is not known (Zou and Kumar, 2018). One potential mechanism could be 2-AG transport to adjacent cells through extracellular vesicles such as micro-vesicles or exosomes. In support of this, a recent study demonstrated that functional eCBs carried on the surface of extracellular vesicles can effectively stimulate eCBR1 signaling (Gabrielli *et al.*, 2015). Further, BSA, a high affinity lipid protein, present in the neural differentiation medium as a component of FBS, might also help in transporting 2-AG to the adjacent NPCs to promote neuronal differentiation.

5.3. Continued passaging of NPCs is a novel alternate model to study the aPKC-CBP-Mgll pathway

The aPKC-CBP pathway is a signaling-directed epigenetic pathway that can be activated in response to various environmental stimuli. Previous work from our lab has demonstrated that metformin can activate the aPKC-CBP pathway both *in vivo* and *in vitro* (Wang *et al.*, 2012; Fatt *et al.*, 2015). Another recent publication from our lab showed that this pathway is activated in the murine hippocampus during aging from 3 months to 6 months (Gouveia *et al.*, 2016). My results now show that continued passaging of NPCs in culture can also activate the aPKC-CBP pathway to repress Mgll expression.

Interestingly, despite a variation in total aPKC levels during continued passaging, the active form of aPKC, pT410/403-aPKC, was consistently upregulated in the P5 NPCs relative to their P2 counterparts, irrespective of the genotype (**Figure 7 C**).

While the exact mechanism that mediates an intrinsic activation of the aPKC-CBP pathway in the late passage NPCs is not known, it can be speculated that stress of continued passaging underlies this effect and triggers aPKC-CBP pathway activation to drive terminal differentiation of NPCs. Interestingly, the aPKC-CBP pathway lies downstream of AMP-activated protein kinase (AMPK) (Fatt *et al.*, 2015) and AMPK activation in response to stress, which has been reported previously (Lin *et al.*, 2017), may explain these effects.

Intriguingly, I also observed that the P5 NPCs exhibit a higher amount of Mgll as compared to the early passage P2 NPCs, irrespective of the genotype and increased aPKC activity (**Figure 7 A**). This suggests that other mechanisms, in addition to the aPKC-CBP pathway, may regulate Mgll protein levels during passaging. One potential explanation might be a highly active Mgll protein degradation machinery in the early passage (P2) NPCs that is rendered inactive in the late passage (P5) NPCs. However, what drives rapid Mgll degradation in the P2 NPCs is uncertain and requires further investigation. Interestingly, a recent review paper compared three independent RNA-seq and microarray datasets from adult NPCs and concluded that Mgll protein is highly expressed in quiescent NPCs, but not in highly-proliferative 'activated' NPCs (Hamilton and Fernandes, 2018). This provides peripheral evidence to support our observations that early passaged NPCs (considered to be highly proliferative) express minimal Mgll, while late passaged NPCs (with reduced capability to form neurospheres) show robust Mgll expression.

While metformin can successfully activate the aPKC-CBP pathway to promote NPC differentiation, the late passage NPC model represents a better system to assess the role of aPKC-CBP mediated Mgll repression in regulating NPC proliferation versus differentiation. This is because metformin not only acts through the aPKC-CBP pathway to drive NPC differentiation, but also promotes NPC proliferation via enhanced expression of the p53 gene homolog, transcriptionally active protein 73 (TAp73) (Fatt *et al.*, 2015). Therefore, use of the late passage model circumvents the off-target effects of metformin stimulation and enables the simultaneous assessment of NPC proliferation versus differentiation regulated by an intrinsically active aPKC-CBP pathway.

5.4. Mgll promotes NPC proliferation at the expense of neuronal differentiation

Mgll activity shifts the balance between two critical bioactive lipid molecules: 2-AG and ARA in the brain. Interesting, ARA-GPR40 signaling is known to promote NPC proliferation in the primate brain (Boneva and Yamashima, 2012; Yamashima, 2012), while 2-AG-eCBR signaling has been shown to enhance neuronal differentiation of adult NPCs (Díaz-Alonso *et al.*, 2012; Xapelli *et al.*, 2013; Compagnucci *et al.*, 2013). In agreement with these earlier studies, my research identifies Mgll as a critical switch between NPC proliferation and differentiation by altering 2-AG versus ARA levels. This is intriguing as it indicates that two bioactive lipid signaling pathways that differentially regulate NPC proliferation and differentiation are controlled by a single lipase, whose gene expression is in turn regulated by a signaling-directed epigenetic pathway, the aPKC-CBP pathway.

While my results strongly suggest that Mgll accumulation in the CBPS436A and 3xTg NPCs reduces 2-AG while increasing ARA levels to promote NPC proliferation at the expense of neuronal differentiation, future work would require a direct assessment of levels of 2-AG and ARA in differentiating CBPS436A and 3xTg NPCs to confirm the altered lipid compositions.

5.5. The aPKC-CBP-Mgll pathway is impaired in 3xTg NPCs

Reduced aPKC activation has been extensively reported in AD (Masliah *et al.*, 1991; Moore *et al.*, 1998; Etcheberrigaray *et al.*, 2004; Tan *et al.*, 2010; Talman *et al.*, 2016) and Mgll has been associated with AD pathophysiology (Chen *et al.*, 2012). However, a direct link between these two processes has never been considered. In this regard, my study for the first time provides evidence to support a causal link between reduced aPKC activation and Mgll accumulation in AD, thereby providing a mechanistic insight into the contribution of aPKC inactivation in AD predisposition. My work argues that impairment of the aPKC-CBP mediated Mgll repression increases Mgll levels that prevents neurogenesis, and potentially contributes to AD predisposition and AD-associated cognitive decline.

Although I don't have a direct evidence showing increased CBP binding to Mgll promoter in 3xTg NPCs, I show that reactivation of the aPKC-CBP mediated Mgll repression at three molecular levels: aPKC, CBPS436 and Mgll, all mitigate the neuronal differentiation deficits of 3xTg NPCs to the same extent. This strongly argues that targeting the aPKC-CBP mediated Mgll repression in AD has the capability to rescue impaired neurogenesis and potentially improve cognition. Interestingly, treatment with eCBR2 agonist (JWH133) but not eCBR1 agonist (ACEA),

rescued the 3xTg NPC differentiation deficits. A potential explanation for this could be increased eCBR2 expression in 3xTg, as is often observed under neuropathological conditions such as AD (Lu and Mackie, 2015; Di Marzo *et al.*, 2015). While eCBR2 signaling is well-known for its neuroprotective functions, a recent study demonstrated that eCBR2 activation can also promote post-stroke neurogenesis (Bravo-Ferrer *et al.*, 2017), thus supporting the neurogenic potential of eCBR2 signaling.

Since effects of metformin on neurodegenerative disease-related cognitive decline have been controversial (Ng *et al.*, 2014; Moore *et al.*, 2013), a delineation of the molecular pathway through which metformin acts is imperative. The identification of Mgll as a biomarker to screen a subpopulation of AD patients for effective metformin treatment will have potential to bring personalised medicine to clinical practice in the near future.

6. Conclusion

In summary, I have shown that activation of the aPKC-CBP pathway by metformin, continued passaging and aging, represses Mgll expression to promote neuronal differentiation of adult NPCs. I have also demonstrated that impairment of aPKC-CBP mediated Mgll repression in the CBPS436A and 3xTg AD NPCs is associated with enhanced NPC proliferation at the expense of neuronal differentiation. These findings indicate that Mgll acts as a switch to differentially regulate NPC proliferation and differentiation by altering ARA-GPR40 versus 2-AG-eCBR signaling. Thus, my study underscores the significance of aPKC-CBP mediated Mgll repression in regulating normal NPC function and suggests that impairment of this pathway may contribute to AD predisposition.

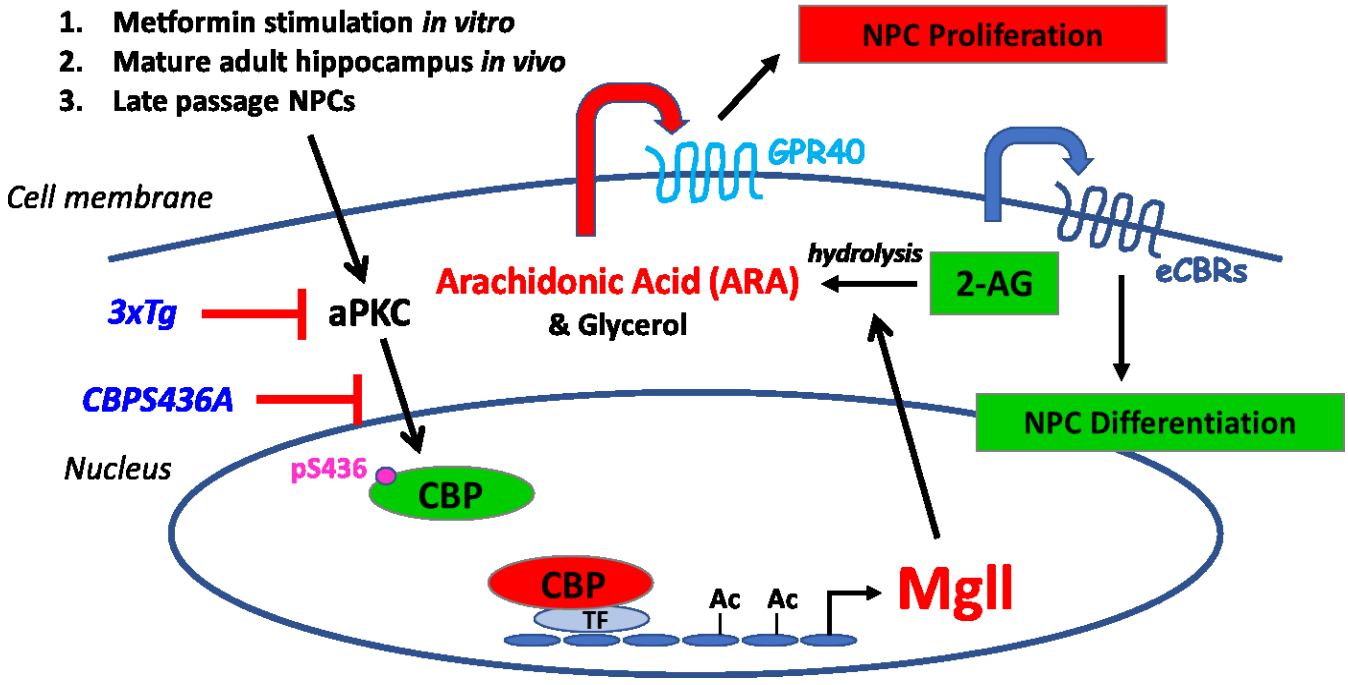

Diagram 2: Schematic summary of thesis.

7. References

5xFAD | Alzforum. (n.d.). Retrieved May 14, 2018, from http://www.alzforum.org/research-models/5xfad

Altman J and Das GD. (1965) Autoradiographic and histological evidence of postnatal hippocampal neurogenesis in rats. J Comp Neurol. 124: 319-335.

Alzheimer A. Uber eine eigenartige Erkrankung der Hirnrinde. Allg Zeitschrift Psychiatr 1907; 64: 146–148.

Arendash GW, King DL, Gordon MN, Morgan D, Hatcher JM, Hope CE and Diamond DM. (2001) Progressive, age-related behavioral impairments in transgenic mice carrying both mutant amyloid precursor protein and presenilin-1 transgenes. Brain Res. 891(1-2): 42-53.

Aso E and Ferrer I. (2016) CB2 Cannabinoid Receptor as Potential Target against Alzheimer's Disease. Front. Neurosci. 10: 243.

Beltz BS, Tlusty MF, Benton JL and Sandeman DC. (2007) Omega-3 fatty acids upregulate adult neurogenesis. Neurosci Lett. 415(2): 154-158.

Benito C, Núñez E, Tolón RM, Carrier EJ, Rábano A, Hillard CJ and Romero J. (2003) Cannabinoid CB2 receptors and fatty acid amide hydrolase are selectively overexpressed in neuritic plaque-associated glia in Alzheimer's disease brains. J Neurosci. 23: 11136-11141.

Bergmann O, Liebl J, Bernard S, Alkass K, Yeung MS, Steier P, Kutschera W, Johnson L, Landén M, Druid H, Spalding KL and Frisén J. (2012) The age of olfactory bulb neurons in humans. Neuron 74: 634-639.

Bieberich E. (2012) It's a lipid's world: bioactive lipid metabolism and signaling in neural stem cell differentiation. Neurochem Res. 37(6): 1208-29.

Billings LM, Oddo S, Green KN, McGaugh JL and LaFerla FM. (2005) Intraneuronal Abeta causes the onset of early Alzheimer's disease-related cognitive deficits in transgenic mice. Neuron. 45(5): 675-688.

Blankman JL, Simon GM and Cravatt BF. (2007) A comprehensive profile of brain enzymes that hydrolyze the endocannabinoid 2-arachidonoylglycerol. Chem Biol. 14(12): 1347-1356.

Boekhoorn K, Joels M and Lucassen PJ. (2006). Increased proliferation reflects glial and vascular-associated changes, but not neurogenesis in the presenile Alzheimer hippocampus. Neurobiol Dis. 24: 1-14.

Boldrini M, Fulmore CA, Tartt AN, Simeon LR, Pavlova I, Poposka V, Rosoklija GB, Stankov A, Arango V, Dwork AJ, Hen R and Mann JJ. (2018). Human hippocampal neurogenesis persists throughout aging. Cell Stem Cell 22(4): 589-599.e5.

Bond AM, Ming G and Song H. (2015) Adult Mammalian Neural Stem Cells and Neurogenesis: Five Decades Later. Cell Stem Cell. 17(4): 385-395.

Boneva NB and Yamashima T. (2012) New insights into 'GPR40-CREB interaction in adult neurogenesis' specific for primates. Hippocampus 22: 896e905.

Bonnet AE and Marchalant Y. (2015) Potential Therapeutic Contributions of the Endocannabinoid System towards Aging and Alzheimer's Disease. Aging and Disease 6(5): 400-405.

Bottino CM, Castro CC, Gomes RL, Buchpiguel CA, Marchetti RL and Neto MR. (2002) Volumetric MRI measurements can differentiate Alzheimer's disease, mild cognitive impairment, and normal aging. Int Psychogeriatr. 14(1): 59-72.

Bravo-Ferrer I, Cuartero MI, Zarruk JG, Pradillo JM, Hurtado O, Romera VG, Díaz-Alonso J, García-Segura JM, Guzmán M, Lizasoain I, Galve-Roperh I and Moro MA. (2017) Cannabinoid Type-2 Receptor Drives Neurogenesis and Improves Functional Outcome After Stroke. Stroke. 48(1): 204-212.

Bu G. (2009) Apolipoprotein E and its receptors in Alzheimer's disease: pathways, pathogenesis and therapy. Nat Rev Neurosci 10: 333-344.

Carroll JC, Rosario ER, Kreimer S, Villamagna A, Gentzschein E, Stanczyk FZ and Pike CJ. (2010) Sex differences in β-amyloid accumulation in 3xTg-AD mice: role of neonatal sex steroid hormone exposure. Brain Res. 1366: 233-245.

Caselli RJ, Beach TG, Yaari R and Reiman EM. (2006) Alzheimer's disease a century later. J Clin Psychiatry 67(11): 1784-1800.

Cassano T, Calcagnini S, Pace L, De Marco F, Romano A and Gaetani S. (2017) Cannabinoid Receptor 2 Signaling in Neurodegenerative Disorders: From Pathogenesis to a Promising Therapeutic Target. Front Neurosci. 11: 30.

Chambers LW, Bancej C and McDowell I (2016). Prevalence and Monetary Costs of Dementia in Canada. Alzheimer Society of Canada. Available at http://alzheimer.ca/sites/default/files/files/national/statistics/prevalenceandcostsofdementia_en.pdf

Chanda PK, Gao Y, Mark L, Btesh J, Strassle BW, Lu P, Piesla MJ, Zhang M, Bingham B, Uveges A, Kowal D, Garbe D, Kouranova EV, Ring RH, Bates B, Pangalos MN, Kennedy JD, Whiteside GT

and Samad TA. (2010) Monoacylglycerol lipase activity is a critical modulator of the tone and integrity of the endocannabinoid system. Mol Pharmacol. 78(6): 996-1003.

Chen R, Zhang J, Wu Y, Wang D, Feng G, Tang Y, Teng Z and Chen C. (2012) Monoacylglycerol Lipase Is a Therapeutic Target for Alzheimer's Disease. Cell Reports 2: 1329-1339.

Chorna NE, Santos-Soto IJ, Carballeira NM, Morales JL, de la Nuez J, Catala-Valentin A, Chornyy AP, Vazquez-Montes A and De Ortiz SP (2013) Fatty acid synthase as a factor required for exercise-induced cognitive enhancement and dentate gyrus cellular proliferation. PLoS One 8(11): e77845.

Codega P, Silva-Vargas V, Paul A, Maldonado-Soto AR, Deleo AM, Pastrana E and Doetsch F. (2014). Prospective identification and purification of quiescent adult neural stem cells from their *in vivo* niche. Neuron 82(3): 545-559.

Compagnucci C, Di Siena S, Bustamante MB, Di Giacomo D, Di Tommaso M, Maccarrone M, Grimaldi P and Sette C. (2013) Type-1 (CB1) cannabinoid receptor promotes neuronal differentiation and maturation of neural stem cells. PLoS One. 8(1): e54271.

Cummings JL. (2004). Alzheimer's disease. N Engl J Med. 351(1): 56-67.

Di Marzo V and De Petrocellis L. (2012) Why do cannabinoid receptors have more than one endogenous ligand? Philos Trans R Soc Lond B Biol Sci. 367(1607): 3216-3228.

Di Marzo V, Stella N and Zimmer A (2015). Endocannabinoid signalling and the deteriorating brain. Nat Rev Neurosci. 16(1): 30-42.

Díaz-Alonso J, Aguado T, Wu CS, Palazuelos J, Hofmann C, Garcez P, Guillemot F, Lu HC, Lutz B, Guzmán M and Galve-Roperh I. (2012) The CB(1) cannabinoid receptor drives corticospinal motor neuron differentiation through the Ctip2/Satb2 transcriptional regulation axis. J Neurosci. 32(47): 16651-16665.

Dinh TP, Carpenter D, Leslie FM, Freund TF, Katona I, Sensi SL, Kathuria S and Piomelli D. (2002) Brain monoglyceride lipase participating in endocannabinoid inactivation. Proc Natl Acad Sci U S A. 99(16): 10819-10824.

Eriksson PS, Perfilieva E, Bjork-Eriksson T, Alborn AM, Nordborg C, Peterson DA and Gage FH. (1998) Neurogenesis in the adult human hippocampus. Nat Med. 4(11): 1313-1317.

Ernst A, Alkass K, Bernard S, Salehpour M, Perl S, Tisdale J, Possnert G, Druid H, Frisen J. (2014) Neurogenesis in the striatum of the adult human brain. Cell 156: 1072-1083.

Etcheberrigaray R, Tan M, Dewachter I, Kuipéri C, Van der Auwera I, Wera S, Qiao L, Bank B, Nelson TJ, Kozikowski AP, Van Leuven F and Alkon DL (2004). Therapeutic effects of PKC

activators in Alzheimer's disease transgenic mice. Proc Natl Acad Sci U S A. 101(30): 11141-11146.

Fatt M, Hsu K, He L, Wondisford F, Miller FD, Kaplan DR, Wang J. (2015) Metformin acts on two different molecular pathways to enhance adult neural precursor proliferation/self-renewal and differentiation. Stem Cell Reports 5: 1-8.

Feng R, Rampon C, Tang YP, *et al.* (2001) Deficient neurogenesis in forebrain-specific presenilin-1 knockout mice is associated with reduced clearance of hippocampal memory traces. Neuron 32: 911-926.

Foley P. (2010) Lipids in Alzheimer's disease: a century-old story. Biochim Biophys Acta 1801: 750-753.

Fonseca BM, Costa MA, Almada M, Correia-da-Silva G, Teixeira NA. (2013) Endogenous cannabinoids revisited: a biochemistry perspective. Prostaglandins Other Lipid Mediat. 102-103: 13-30.

Forstl H and Kurz A. (1999) Clinical features of Alzheimer's disease. Eur Arch Psychiatry Clin Neurosci 249(6): 288-290.

Fowler CJ. (2012) Monoacylglycerol lipase – a target for drug development? Br J Pharmacol 166(5): 1568-1585.

Fraser T, Tayler H and Love S. (2010) Fatty acid composition of frontal, temporal and parietal neocortex in the normal human brain and in Alzheimer's disease. Neurochem Res 35(3): 503-513.

Gabrielli M, Battista N, Riganti L, Prada I, Antonucci F, Cantone L, Matteoli M, Maccarrone M and Verderio C. (2015) Active endocannabinoids are secreted on extracellular membrane vesicles. EMBO Rep. 16(2): 213-20.

Galve-Roperh I, Chiurchiù V, Díaz-Alonso J, Bari M, Guzmán M, Maccarrone M. (2013) Cannabinoid receptor signaling in progenitor/stem cell proliferation and differentiation. Prog Lipid Res. 52(4): 633-50.

Gan L, Qiao S, Lan X, Chi L, Luo C, Lien L, Yan Q, and Liu R. (2008) Neurogenic responses to amyloid-beta plaques in the brain of Alzheimer's disease-like transgenic (pPDGF-APPSw, Ind) mice. Neurobiol Dis 29(1): 71-80.

Gao Y, Vasilyev DV, Goncalves MB, Howell FV, Hobbs C, Reisenberg M, Shen R, Zhang MY, Strassle BW, Lu P, Mark L, Piesla MJ, Deng K, Kouranova EV, Ring RH, Whiteside GT, Bates B, Walsh FS, Williams G, Pangalos MN, Samad TA and Doherty P. (2010) Loss of retrograde

endocannabinoid signaling and reduced adult neurogenesis in diacylglycerol lipase knock-out mice. J Neurosci. 30(6): 2017-2024.

Goncalves MB, Suetterlin P, Yip P, Molina-Holgado F, Walker DJ, Oudin MJ, Zentar MP, Pollard S, Yáñez-Muñoz RJ, Williams G, Walsh FS, Pangalos MN and Doherty P. (2008) A diacylglycerol lipase-CB2 cannabinoid pathway regulates adult subventricular zone neurogenesis in an age-dependent manner. Mol Cell Neurosci. 38(4): 526-536.

Gouveia A, Hsu K, Niibori Y, Seegobin M, Cancino GI, He L, Wondisford FE, Bennett S, Lagace D, Frankland PW and Wang J. (2016) The aPKC-CBP pathway regulates adult hippocampal neurogenesis in an age-dependent manner. Stem Cell Reports. 7(4): 719-734.

Grabner GF, Eichmann TO, Wagner B, Gao Y, Farzi A, Taschler U, Radner FPW, Schweiger M, Lass A, Holzer P, Zinser E, Tschöp MH, Yi C and Zimmermann R. (2016) Deletion of Monoglyceride Lipase in Astrocytes Attenuates Lipopolysaccharide-induced Neuroinflammation. J Biol Chem. 291(2): 913-923.

Hamilton LK, Aumont A, Julien C, Vadnais A, Calon F and Fernandes KJ. (2010) Widespread deficits in adult neurogenesis precede plaque and tangle formation in the 3xTg mouse model of Alzheimer's disease. Euro J Neurosci. 32(6): 905-920.

Hamilton LK, Dufresne M, Joppe SE, Petryszyn S, Aumont A, Calon F, Barnabe-Heider F, Furtos A, Parent M, Chaurand P and Fernandes KJL. (2015) Aberrant lipid metabolism in the forebrain niche suppresses adult neural stem cell proliferation in an animal model of Alzheimer's disease. Cell Stem Cell 17(4): 397-411.

Hamilton LK and Fernandes KJL. (2018) Neural stem cells and adult brain fatty acid metabolism: Lessons from the 3xTg model of Alzheimer's disease. Biol Cell. 110(1): 6-25.

Hall AM and Roberson ED. (2012) Mouse Models of Alzheimer's Disease. Brain Res Bull. 88(1): 3-12.

Haughey NJ, Nath A, Chan SL, Borchard AC, Rao MS and Mattson MP (2002). Disruption of neurogenesis by amyloid beta- peptide, and perturbed neural progenitor cell homeostasis, in models of Alzheimer's disease. J Neurochem. 83(6): 1509-1524.

He C, Qu X, Cui L, Wang J and Kang JX. (2009) Improved spatial learning performance of fat-1 mice is associated with enhanced neurogenesis and neuritogenesis by docosahexaenoic acid. Proc Natl Acad Sci U S A. 106(27): 11370-11375.

Hermanson DJ, Gamble-George JC, Marnett LJ and Patel S. (2014) Substrate-selective COX-2 inhibition as a novel strategy for therapeutic endocannabinoid augmentation. Trends Pharmacol Sci. 35(7): 358-367.

Holcomb L, Gordon MN, McGowan E, Yu X, Benkovic S, Jantzen P, Wright K, Saad I, Mueller R, Morgan D, Sanders S, Zehr C, O'Campo K, Hardy J, Prada CM, Eckman C, Younkin S, Hsiao K and Duff K. (1998) Accelerated Alzheimer-type phenotype in transgenic mice carrying both mutant amyloid precursor protein and presenilin 1 transgenes. Nat Med. 4(1): 97-100.

Hsiao K, Chapman P, Nilsen S, Eckman C, Harigaya Y, Younkin S, Yang F and Cole G. (1996) Correlative memory deficits, Abeta elevation, and amyloid plaques in transgenic mice. Science. 274(5284): 99-102.

Hussain G, Schmitt F, Loeffler JP and Gonzalez de Aguilar JL. (2013) Fatting the brain: a brief of recent research. Front Cell Neurosci. 7: 144.

Imayoshi I, Sakamoto M, Ohtsuka T, Takao K, Miyakawa T, Yamaguchi M, Mori K, Ikeda T, Itohara S and Kageyama R. (2008) Roles of continuous neurogenesis in the structural and function integrity of the adult forebrain. Nat Neurosci. 11(10): 1153-1161.

Jaenisch R and Bird A. (2003) Epigenetic regulation of gene expression: how the genome integrates intrinsic and environmental signals. Nat Genet. 33 Suppl.: 245–254.

Jawhar S, Trawicka A, Jenneckens C, Bayer TA and Wirths O. (2012) Motor deficits, neuron loss, and reduced anxiety coinciding with axonal degeneration and intraneuronal Aβ aggregation in the 5XFAD mouse model of Alzheimer's disease. Neurobiol Aging. 33(1): 196.e29-40.

Jawahar S. (2011) The 5XFAD mouse model: a tool for genetic modulation of Alzheimer’s disease pathology (Doctoral dissertation). Retrieved from the GGNB - Göttinger Graduiertenschule für Neurowissenschaften, Biophysik und molekulare Biowissenschaften database. Available at https://ediss.uni-goettingen.de/handle/11858/00-1735-0000-0006-B5D8-7

Jessberger S and Parent JM (2015). Epilepsy and Adult Neurogenesis. Cold Spring Harb. Perspect Biol. 7: a020677.

Jin K, Galvan V, Xie L, Mao XO, Gorostiza OF, Bredesen DE and Greenberg DA. (2004a) Enhanced neurogenesis in Alzheimer’s disease transgenic (PDGF APPSw,Ind) mice. PNAS 101(36): 13363-13367.

Jin K, Xie L, Kim SH, Parmentier-Batteur S, Sun Y, Mao XO, Childs J and Greenberg DA. (2004b) Defective Adult Neurogenesis in CB1 Cannabinoid Receptor Knockout Mice. Mol Pharmacol. 66(2): 204-208.

Jin K, Peel AL, Mao XO, Xie L, Cottrell BA, Henshall DC and Greenberg DA. (2004c) Increased hippocampal neurogenesis in Alzheimer’s disease. Proc Natl Acad Sci U S A. 101(1): 343-347.

Karch CM and Goate AM. (2015) Alzheimer’s disease risk genes and mechanisms of disease pathogenesis. Biol Psychiatry. 77(1): 43-51.

Kang JX, Wan J and He C. (2014) Concise Review: Regulation of Stem Cell Proliferation and Differentiation by Essential Fatty Acids and Their Metabolites. Stem Cells. 32(5):1092-8.

Kawakita E, Hashimoto M and Shido O. (2006) Docosahexaenoic acid promotes neurogenesis in vitro and *in vivo*. Neuroscience. 139(3): 991-997.

Kempermann G, Kuhn HG and Gage FH. (1997) More hippocampal neurons in adult mice living in an enriched environment. Nature. 386(6624): 493-495.

Kempermann G, Gage FH, Aigner L, Song H, Curtis MA, Thuret S, Kuhn HG, Jessberger S, Frankland PW, Cameron HA, Gould E, Hen R, Abrous DN, Toni N, Schinder AF, Zhao X, Lucassen PJ and Frisén J. (2018) Human Adult Neurogenesis: Evidence and Remaining Questions. Cell Stem Cell. 23(1): 25-30.

Kendall DA and Yudowski GA. (2017) Cannabinoid Receptors in the Central Nervous System: Their Signaling and Roles in Disease. Front Cell Neurosci. 10:294.

Khanapure SP, Garvey DS, Janero DR and Letts LG. (2007) Eicosanoids in inflammation: biosynthesis, pharmacology, and therapeutic frontiers. Curr Top Med Chem. 7(3): 311-340.

Knobloch M and Jessberger S. (2017) Metabolism and neurogenesis. Curr Opin Neurobiol. 42: 45-52.

Knobloch M. (2017) The Role of Lipid Metabolism for Neural Stem Cell Regulation. Brain Plast. 3(1): 61-71.

Knobloch M, Braun SM, Zurkirchen L, von Schoultz C, Zamboni N, Arauzo-Bravo MJ, Kovacs WJ, Karalay O, Suter U, Machado RA, Roccio M, Lutolf MP, Semenkovich CF and Jessberger S. (2013) Metabolic control of adult neural stem cell activity by Fasn-dependent lipogenesis. Nature. 493(7431): 226-230.

Kohler SJ, Williams NI, Stanton GB, Cameron JL, and Greenough WT. (2011). Maturation time of new granule cells in the dentate gyrus of adult macaque monkeys exceeds six months. Proc Natl Acad Sci USA. 108: 10326-10331.

Kuhn HG, Eisch AJ, Spalding K and Peterson DA (2016) Detection and Phenotypic Characterization of Adult Neurogenesis. Cold Spring Harb Perspect Biol. 8(3): a025981.

Lane CA, Hardy J and Schott JM. (2017) Alzheimer's Disease. Eur J Neurol. 25(1): 59-70.

Lange-Asschenfeldt C and Kojda G. (2008) Alzheimer's disease, cerebrovascular dysfunction and the benefits of exercise: from vessels to neurons. Exp Gerontol. 43(6): 499-504.

Lardenoije R, Iatrou A, Kenis G, Kompotis K, Steinbusch HW, Mastroeni D, Coleman P, Lemere CA, Hof PR, van den Hove DL and Rutten BP. (2015) The epigenetics of aging and neurodegeneration. Prog Neurobiol. 131: 21-64.

Lazarov O and Marr RA (2010). Neurogenesis and Alzheimer's disease: At the crossroads. Exp Neurol. 223(2): 267-281.

Li B, Yamamori H, Tatebayashi Y, Shafit-Zagardo B, Tanimukai H, Chen S, Iqbal K and Grundke-Iqbal I. (2008) Failure of Neuronal Maturation in Alzheimer Disease Dentate Gyrus. J Neuropathol Exp Neurol. 67(1): 78-84.

Lichtenwalner RJ and Parent JM (2006). Adult neurogenesis and the ischemic forebrain. J Cereb Blood Flow Metab. 26(1): 1-20.

Lin CH, Cheng YC, Nicol CJ, Lin KH, Yen CH and Chiang MC. (2017) Activation of AMPK is neuroprotective in the oxidative stress by advanced glycosylation end products in human neural stem cells. Exp Cell Res. 359(2): 367-373.

Lindsay J, Laurin D, Verreault R, Hebert R, Helliwell B, Hill GB, McDowell I. (2002) Risk factors for Alzheimer's disease: a prospective analysis from the Canadian Study of Health and Aging. Am J Epidemiol. 156(5): 445-453.

Liu Q and Zhang J. (2014) Lipid metabolism in Alzheimer’s disease. Neurosci Bull 30(2): 331-345.

Llorens-Bobadilla E, Zhao S, Baser A, Saiz-Castro G, Zwadlo K and Martin-Villalba A. (2015) Single-cell transcriptomics reveals a population of dormant neural stem cells that become activated upon brain injury. Cell Stem Cell 17(3): 329-340.

Lois C and Alvarez-Buylla A. (1993) Proliferating subventricular zone cells in the adult mammalian forebrain can differentiate into neurons and glia. Proc Natl Acad Sci U S A. 90(5): 2074-2077.

Long JZ, Li W, Booker L, Burston JJ, Kinsey SG, Schlosburg JE, Pavón FJ, Serrano AM, Selley DE, Parsons LH, Lichtman AH and Cravatt BF. (2009) Selective blockade of 2-arachidonoylglycerol hydrolysis produces cannabinoid behavioral effects. Nat Chem Biol. 5(1): 37-44.

Lopez-Toledano MA and Shelanski ML (2007). Increased neurogenesis in young transgenic mice overexpressing human APP (Sw, Ind). J Alzheimers Dis. 12(3): 229-240.

Lu H and Mackie K (2015). An introduction to the endogenous cannabinoid system. Biol Psychiatry. 79(7): 516–525.

Ma DK, Marchetto MC, Guo JU, Ming GL, Gage FH and Song H. (2010) Epigenetic choreographers of neurogenesis in the adult mammalian brain. Nat Neurosci. 13(11): 1338-44.

Maccarrone M, Guzmán M, Mackie K, Doherty P and Harkany T. (2014) Programming of neural cells by (endo)cannabinoids: from physiological rules to emerging therapies. Nat Rev Neurosci. 15(12): 786-801.

Maekawa M, Takashima N, Matsumata M, Ikegami S, Kontani M, Hara Y, Kawashima H, Owada Y, Kiso Y, Yoshikawa T, Inokuchi K and Osumi N. (2009) Arachidonic acid drives postnatal neurogenesis and elicits a beneficial effect on prepulse inhibition, a biological trait of psychiatric illnesses. PLoS One. 4(4): e5085.

Marsicano G, Goodenough S, Monory K, Hermann H, Eder M, Cannich A, Azad SC, Cascio MG, Gutiérrez SO, van der Stelt M, López-Rodriguez ML, Casanova E, Schütz G, Zieglgänsberger W, Di Marzo V, Behl C, Lutz B. (2003) CB1 cannabinoid receptors and on-demand defense against excitotoxicity. Science 302(5642): 84-88.

Marlatt MW, Hoozemans JJM, Veerhuis R and Lucassen PJ. (2009) Alzheimer's Disease and Adult Neurogenesis—Are Endogenous Stem Cells Part of the Solution? US Neurol. 5(1): 12-14.

Marques SC, Oliveira CR, Pereira CM and Outeiro TF. (2011) Epigenetics in neurodegeneration: a new layer of complexity. Prog Neuropsychopharmacol Biol Psychiatry. 35(2): 348-355.

Masliah E, Cole GM, Hansen LA, Mallory M, Albright T, Terry RD and Saitoh T. (1991) Protein kinase C alteration is an early biochemical marker in Alzheimer's disease. J Neurosci. 11(9): 2759-2767.

Mega MS, Cummings JL, Fiorello T and Gornbein J. (1996) The spectrum of behavioral changes in Alzheimer's disease. Neurology 46(1): 130-135.

Metaxas A and Kempf SJ. (2016) Neurofibrillary tangles in Alzheimer's disease: elucidation of the molecular mechanism by immunohistochemistry and tau protein phospho-proteomics. Neural Regen Res. 11(10): 1579-1581.

Moore EM, Mander AG, Ames D, Kotowicz MA, Carne RP, Brodaty H, Woodward M, Boundy K, Ellis KA, Bush AI, Faux NG, Martins R, Szoeke C, Rowe C, Watters DA; AIBL Investigators. (2013) Increased risk of cognitive impairment in patients with diabetes is associated with metformin. Diabetes Care. 36(10): 2981-2987.

Moore P, White J, Christiansen V and Grammes, P. (1998) Protein kinase C-zeta activity but not level is decreased in Alzheimer's disease microvessels. Neurosci Lett. 254(1): 29-32.

Mota SI, Ferreira IL, Rego AC. (2014) Dysfunctional synapse in Alzheimer's disease - A focus on NMDA receptors. Neuropharmacology 76: 16-26.

Mu Y and Gage FH. (2011) Adult hippocampal neurogenesis and its role in Alzheimer's disease. Mol Neurodegener. 6: 85.

Mulvihill MM and Nomura DK. (2013) Therapeutic Potential of Monoacylglycerol Lipase Inhibitors. Life Sci. 92(8-9): 492-497.

Ng TP, Feng L, Yap KB, Lee TS, Tan CH and Winblad B. (2014) Long-term metformin usage and cognitive function among older adults with diabetes. J Alzheimers Dis. 41(1): 61-68.

Nomura DK, Morrison BE, Blankman JL, Long JZ, Kinsey SG, Marcondes MC, Ward AM, Hahn YK, Lichtman AH, Conti B and Cravatt BF. (2011) Endocannabinoid hydrolysis generates brain prostaglandins that promote neuroinflammation. Science 334(6057): 809-813.

Oakley H, Cole SL, Logan S, Maus E, Shao P, Craft J, Guillozet-Bongaarts A, Ohno M, Disterhoft J, Van Eldik L, Berry R, Vassar R. (2006) Intraneuronal beta-amyloid aggregates, neurodegeneration, and neuron loss in transgenic mice with five familial Alzheimer's disease mutations: potential factors in amyloid plaque formation. J Neurosci. 26(40): 10129-10140.

Oddo S, Caccamo A, Kitazawa M, Tseng BP, LaFerla FM. (2003a) Amyloid deposition precedes tangle formation in a triple transgenic model of Alzheimer's disease. Neurobiol Aging. 24: 1063-1070.

Oddo S, Caccamo A, Shepherd JD, Murphy MP, Golde TE, Kayed R, Metherate R, Mattson MP, Akbari Y, LaFerla FM. (2003b) Triple-transgenic model of Alzheimer's disease with plaques and tangles: intracellular Abeta and synaptic dysfunction. Neuron 39(3): 409-421.

Pacher P, Batkai S, and Kunos G. (2006) The Endocannabinoid System as an Emerging Target of Pharmacotherapy. Pharmacol Rev. 58(3): 389-462.

Palazuelos J, Aguado T, Egia A, Mechoulam R, Guzman M and Galve-Roperh I. (2006) Non-psychoactive CB2 cannabinoid agonists stimulate neural progenitor proliferation. FASEB J. 20(13): 2405-2407.

Palazuelos J, Ortega Z, Díaz-Alonso J, Guzmán M and Galve-Roperh I. (2012) CB2 cannabinoid receptors promote neural progenitor cell proliferation via mTORC1 signaling. J Biol Chem. 287(2): 1198-1209.

Panikashvili D, Simeonidou C, Ben-Shabat S, Hanus L, Breuer A, Mechoulam R and Shohami E. (2001) An endogenous cannabinoid (2-AG) is neuroprotective after brain injury. Nature. 413(6855): 527-531.

Perl DP. (2010) Neuropathology of Alzheimer's Disease. Mt Sinai J Med. 77(1): 32-42.

Perry EK, Johnson M, Ekonomou A, Perry RH, Ballard C and Attems J (2012). Neurogenic abnormalities in Alzheimer’s disease differ between stages of neurogenesis and are partly related to cholinergic pathology. Neurobiol Dis. 47(2): 155-162.

Pierce AA and Xu AW. (2010) De novo neurogenesis in adult hypothalamus as a compensatory mechanism to regulate energy balance. J Neurosci. 30(2): 723-730.

Prenderville JA, Kelly AM and Downer EJ. (2015) The role of cannabinoids in adult neurogenesis. Br J Pharmacol 172(16): 3950-3963.

Prince M, Wimo A, Guerchet M, Ali G, Wu Y and Prina M (2015). World Alzheimer Report 2015, The Global Impact of Dementia: An analysis of prevalence, incidence, cost and trends. (2015). Alzheimer's Disease International. Available at https://www.alz.co.uk/research/WorldAlzheimerReport2015.pdf

Puzzo D, Gulisano W, Palmeri A and Arancio O. (2015) Rodent models for Alzheimer's disease drug discovery. Expert Opin Drug Discov. 10(7): 703-711.

Rakic P. (2002) Neurogenesis in adult primate neocortex: an evaluation of the evidence. Nat Rev Neurosci. 3(1): 65-71.

Ramirez BG, Blázquez C, Gómez del Pulgar T, Guzmán M and de Ceballos ML. (2005) Prevention of Alzheimer's disease pathology by cannabinoids: neuroprotection mediated by blockade of microglial activation. J Neurosci. 25(8): 1904-1913.

Rodriguez JJ, Jones VC, Tabuchi M, Allan SM, Knight EM, LaFerla FM, Oddo S and Verkhratsky A. (2008) Impaired adult neurogenesis in the dentate gyrus of a triple transgenic mouse model of Alzheimer's disease. PLoS One 3: e2935.

Rodriguez JJ, Jones VC and Verkhratsky A. (2009) Impaired cell proliferation in the subventricular zone in an Alzheimer's disease model. Neuroreport 20(10): 907-912.

Roses AD. (1996) Apolipoprotein E alleles as risk factors in Alzheimer's disease. Annu Rev Med. 47: 387-400.

Sakayori N, Maekawa M, Numayama-Tsuruta K, Katura T, Moriya T and Osumi N. (2011) Distinctive effects of arachidonic acid and docosahexaenoic acid on neural stem/progenitor cells. Genes Cells. 16(7): 778-790.

Scarmeas N, Hadjigeorgiou GM, Papadimitriou A, Dubois B, Sarazin M, Brandt J, Albert M, Marder K, Bell K, Honig LS, Wegesin D and Stern Y. (2004) Motor signs during the course of Alzheimer disease. Neurology. 63(6): 975-982.

Schlosburg JE, Blankman JL, Long JZ, Nomura DK, Pan B, Kinsey SG, Nguyen PT, Ramesh D, Booker L, Burston JJ, Thomas EA, Selley DE, Sim-Selley LJ, Liu QS, Lichtman AH and Cravatt BF. (2010) Chronic monoacylglycerol lipase blockade causes functional antagonism of the endocannabinoid system. Nat Neurosci. 13(9): 1113-1119.

Schneider A, Schulz-Schaeffer W, Hartmann T, Schulz JB, Simons M. (2006) Cholesterol depletion reduces aggregation of amyloid beta peptide in hippocampal neurons. Neurobiol Dis 23(3): 573-577.

Serrano-Pozo A, Frosch MP, Masliah E and Hyman BT. (2011) Neuropathological alterations in Alzheimer disease. Cold Spring Harb Perspect Med. 1(1): a006189.

Selkoe DJ (2011). Alzheimer's disease. Cold Spring Harb Perspect Biol. 3(7): 15056.

Shevchenko A and Simons K. (2010) Lipidomics: coming to grips with lipid diversity. Nat Rev Mol Cell Biol. 11(8): 593-598.

Shin J, Berg DA, Zhu Y, Shin JY, Song J, Bonaguidi MA, Enikolopov G, Nauen DW, Christian KM, Ming GL and Song H. (2015) Single-Cell RNA-Seq with Waterfall Reveals Molecular Cascades underlying Adult Neurogenesis. Cell Stem Cell 17(3): 360-372.

Shruster A, Melamed E and Offen D. (2010) Neurogenesis in the aged and neurodegenerative brain. Apoptosis 15(11): 1415-1421.

Sorrells SF, Paredes MF, Cebrian-Silla A, Sandoval K, Qi D, Kelley KW, James D, Mayer S, Chang J, Auguste KI, Chang EF, Gutierrez AJ, Kriegstein AR, Mathern GW, Oldham MC, Huang EJ, Garcia-Verdugo JM, Yang Z and Alvarez-Buylla A. (2018). Human hippocampal neurogenesis drops sharply in children to undetectable levels in adults. Nature 555(7696): 377-381.

Spalding KL, Bergmann O, Alkass K, Bernard S, Salehpour M, Huttner HB, Bostrom E, Westerlund I, Vial C, Buchholz BA, Possnert G, Mash DC, Druid H and Frisén J. (2013) Dynamics of hippocampal neurogenesis in adult humans. Cell 153(6): 1219-1227.

Talman V, Pascale A, Jäntti M, Amadio M and Tuominen RK. (2016) Protein Kinase C Activation as a Potential Therapeutic Strategy in Alzheimer's Disease: Is there a Role for Embryonic Lethal Abnormal Vision-like Proteins? Basic Clin Pharmacol Toxicol. 119(2): 149-160.

Tan MG, Chua WT, Esiri MM, Smith AD, Vinters HV and Lai MK. (2010) Genome wide profiling of altered gene expression in the neocortex of Alzheimer's disease. J Neurosci Res. 88(6): 1157-69.

Tanzi RE. (2012) The genetics of Alzheimer disease. Cold Spring Harb Perspect Med. 2: a006296

Tokuda H, Kontani M, Kawashima H, Kiso Y, Shibata H and Osumi N. (2014) Differential effect of arachidonic acid and docosahexaenoic acid on age-related decreases in hippocampal neurogenesis. Neurosci Res. 88: 58-66.

Valor LM, Pulopulos MM, Jimenez-Minchan M, Olivares R, Lutz B and Barco A. (2011) Ablation of CBP in forebrain principal neurons causes modest memory and transcriptional defects and a

dramatic reduction of histone acetylation but does not affect cell viability. J Neurosci. 31(5): 1652–1663.

Van Cauwenberghe C, Van Broeckhoven C and Sleegers K. (2016). The genetic landscape of Alzheimer disease: clinical implications and perspectives. Genet Med. 18(5): 421-30.

Wang J, Gallagher D, DeVito LM, Cancino GI, Tsui D, He L, Keller GM, Frankland PW, Kaplan DR, Miller FD. (2012) Metformin Activates an Atypical PKC-CBP Pathway to Promote Neurogenesis and Enhance Spatial Memory Formation. Cell Stem Cell. 11(1): 23-35.

Wang R, Dineley KT, Sweatt JD and Zheng H. (2004) Presenilin 1 familial Alzheimer's disease mutation leads to defective associative learning and impaired adult neurogenesis. Neuroscience 126(2): 305–312.

Wen PH, Hof PR, Chen X, Gluck K, Austin G, Younkin SG, Younkin LH, DeGasperi R, Gama Sosa MA, Robakis NK, Haroutunian V, Elder GA. (2004) The presenilin-1 familial Alzheimer disease mutant P117L impairs neurogenesis in the hippocampus of adult mice. Exp Neurol. 188(2): 224-237.

Winner B, Kohl Z and Gage FH. (2011) Neurodegenerative disease and adult neurogenesis. J Neurosci 33(6): 1139-1151.

Wippold FJ, Cairns N, Vo K, Holtzman DM and Morris JC. (2008) Neuropathology for the Neuroradiologist: Plaques and Tangles. AJNR Am J Neuroradiol. 29(1): 18-22.

Wong MW, Braidy N, Poljak A, Pickford R, Thambisetty M and Sachdev PS. (2017) Dysregulation of lipids in Alzheimer's disease and their role as potential biomarkers. Alzheimers Dement. 13(7): 810-827.

Wu A, Ying Z and Gomez-Pinilla F. (2008) Docosahexaenoic acid dietary supplementation enhances the effects of exercise on synaptic plasticity and cognition. Neuroscience. 155(3): 751-759.

Xapelli S, Agasse F, Sardà-Arroyo L, Bernardino L, Santos T, Ribeiro FF, Valero J, Bragança J, Schitine C, de Melo Reis RA, Sebastião AM and Malva JO. (2013) Activation of type 1 cannabinoid receptor (CB1R) promotes neurogenesis in murine subventricular zone cell cultures. PLoS One. 8(5): e63529.

Xu Q and Huang Y. (2006) Lipid metabolism in Alzheimer's and Parkinson's disease. Future Lipidology 1(4): 441-453.

Yamashima (2012). 'PUFA-GPR40-CREB signaling' hypothesis for the adult primate neurogenesis. Prog Lipid Res. 51(3): 221-231.

Yu Y, He J, Zhang Y, Luo H, Zhu S, Yang Y, Zhao T, Wu J, Huang Y, Kong J, Tan Q and Li XM. (2009). Increased hippocampal neurogenesis in the progressive stage of Alzheimer's disease phenotype in an APP/PS1 double transgenic mouse model. Hippocampus 19(12): 1247-1253.

Zamarbide M, Etayo-Labiano I, Ricobaraza A, Martínez-Pinilla E, Aymerich MS, Luis Lanciego J, Perez-Mediavilla A and Franco R. (2014) GPR40 activation leads to CREB and ERK phosphorylation in primary cultures of neurons from the mouse CNS and in human neuroblastoma cells. Hippocampus. 24 (7): 733e739.

Zhang C, McNeil E, Dressler L and Siman R. (2007) Long-lasting impairment in hippocampal neurogenesis associated with amyloid deposition in a knock-in mouse model of familial Alzheimer's disease. Exp Neurol. 204: 77-87.

Zhang TY and Meaney, MJ. (2010) Epigenetics and the environmental regulation of the genome and its function. Annu Rev Psychol. 61: 439-466.

Zhao C, Deng W, Gage FH. (2008) Mechanisms and functional implications of adult neurogenesis. Cell. 132(4): 645-660.

Zhou XY, Shibusawa N, Naik K, Porras D, Temple K, Ou H, Kaihara K, Roe MW, Brady MJ and Wondisford FE (2004). Insulin regulation of hepatic gluconeogenesis through phosphorylation of CREB-binding protein. Nat Med. 10(6): 633-637.

Zou S and Kumar U. (2018) Cannabinoid Receptors and the Endocannabinoid System: Signaling and Function in the Central Nervous System. Int J Mol Sci. 19(3).

Appendix

Table 1: shRNA Sequences

Mgll shRNA 1	Forward: 5'-GAG ATC TCC CCG TTA TGA TGA GCT GGC TCT TCA AGA GAG AGC CAG CTC ATC ATA ACG TTT TTA AAG CTT G-3'
	Reverse: 5'-CAA GCT TTA AAA ACG TTA TGA TGA GCT GGC TCT CTC TTG AAG AGC CAG CTC ATC ATA ACG GGG AGA TCT C-3'
Mgll shRNA 2	Forward: 5'-GAG ATC TCC CGT CAA TGC AGA CGG ACA GTT TCA AGA GAA CTG TCC GTC TGC ATT GAC TTT TTA AAG CTT G-3'
	Reverse: 5'-CAA GCT TTA AAA AGT CAA TGC AGA CGG ACA GTT CTC TTG AAA CTG TCC GTC TGC ATT GAC GGG AGA TCT C-3'
Scrambled shRNA	Forward: 5'-CAC CCT TCC TCT CTT TCT CTC CCT TGT GAC GAA TCA CAA GGG AGA GAA AGA GAG GAA G- 3'
	Reverse: 5'-AAA ACT TCC TCT CTT TCT CTC CCT TGT GAT TCG TCA CAA GGG AGA GAA AGA GAG GAA G- 3'

Table 2: Medium and Reagents

Solution	Volume/Weight	Vendor	Catalog #
Serum Free Medium (SFM)			
DMEM (low glucose)	50 mL	Fisher	11885084
Ham's F12	50 mL	Fisher	11765054
30% glucose	2 mL	Sigma-Aldrich	G7021
7.5% sodium bicarbonate	1.5 mL	Sigma-Aldrich	S6014
1M HEPES (pH= 7.4)	0.5 mL	Fisher	BP310100
L-glutamine (200 mM in 0.85% NaCl solution)	1 mL	Lonza	17-605E
Penicillin/streptomycin	1 mL	Fisher	15140122
Enzyme Mix			
Trypsin	40 mg	Sigma-Aldrich	T1005-1G
Hyaluronidase	25 mg	Sigma-Aldrich	H3884-500
Kynurenic acid	3-5 mg	Sigma-Aldrich	K3375-1G
Suspended in 30 mL HBSS (Fisher Scientific, 14175103), mixed on a tube rotator for 30 minutes at 37°C and sterilized using a 0.22 µM syringe filter.			
Trypsin Inhibitor			
Trypsin inhibitor	10 mg	Sigma- Aldrich	T2011-500
Suspended in 15 mL SFM and sterilized using a 0.22 µM syringe filter.			

Table 3: List of Solutions

Solution	Concentration	Vendor	Catalog #
Lysis Buffer pH= 7.4			
Tris-HCl	50mM	Fisher	BP153
NaCl	150mM	Fisher	BP358
Nonidet P-40	0.20%	Sigma-Aldrich	NP40S
Sample Buffer			
SDS	2% w/v	Fisher	BP1311
Glycerol	4% v/v	Fisher	BP229
Tris-HCl	40mM	Fisher	BP153
Bromophenol blue	0.01% w/v	Fisher	B392
β-Mercaptoethanol	1%	Fisher	ICN19024280
Running Buffer			
Tris	25mM	VWR	CABDH4500
Glycine	192mM	Fisher	BP381
SDS	0.1%	Fisher	BP1311
Transfer Buffer			
Tris	192mM	VWR	CABDH4500
Glycine	192mM	Fisher	BP381
Tris Buffered Saline, Tween-20 (TBS-T)			
Tris-HCl	50mM	Fisher	BP153
NaCl	150mM	Fisher	BP358
Tween-20	0.1%	Fisher	BP337